

# micrOMEGAs<sub>3</sub> : a program for calculating dark matter observables

G. Bélanger<sup>1</sup>, F. Boudjema<sup>1</sup>, A. Pukhov<sup>2</sup>, A. Semenov<sup>3</sup>

1) *LAPTH, Univ. de Savoie, CNRS, B.P.110, F-74941 Annecy-le-Vieux, France*

2) *Skobeltsyn Inst. of Nuclear Physics, Moscow State Univ., Moscow 119992, Russia*

3) *Joint Institute of Nuclear research, JINR, 141980 Dubna, Russia*

## Abstract

`micrOMEGAs` is a code to compute dark matter observables in generic extensions of the standard model. This new version of `micrOMEGAs` is a major update which includes a generalization of the Boltzmann equations to accommodate models with asymmetric dark matter or with semi-annihilation and a first approach to a generalization of the thermodynamics of the Universe in the relic density computation. Furthermore a switch to include virtual vector bosons in the final states in the annihilation cross sections or relic density computations is added. Effective operators to describe loop-induced couplings of Higgses to two-photons or two-gluons are introduced and reduced couplings of the Higgs are provided allowing for a direct comparison with recent LHC results. A module that computes the signature of DM captured in celestial bodies in neutrino telescopes is also provided. Moreover the direct detection module has been improved as concerns the implementation of the strange “content” of the nucleon. New extensions of the standard model are included in the distribution.

## 1 Introduction

Cosmological and astrophysical observations have established that the matter content of the Universe is dominated by dark matter (DM). However the nature of this dark matter still needs to be elucidated, therefore searches for dark matter signals are pursued actively. Dark matter observables include the relic density, the elastic scattering cross section on nuclei, the indirect signatures of DM annihilation in the galaxy (leading to photons and antimatter) or DM capture in celestial bodies (leading to neutrinos).

For all these observables, experiments are currently taking data and improved results are expected. The PLANCK satellite has recently determined the DM relic density with a precision of 2% [1]. Direct detection experiments such as DAMA [2], CDMS [3] CoGeNT [4] and CRESST [5] have found events that could be compatible with DM in the range 5-30 GeV, these are however incompatible with the upper limits on spin independent DM interactions with nuclei set by Xenon100 [6]. Furthermore COUPP [7], Picasso [8] and Xenon100 [6] have set limits on spin dependent interactions. Larger direct detection projects with ton scale detectors are planned, e.g. Xenon, and should improve by more than one order of magnitude the current sensitivity. Indirect detection experiments are measuring the spectrum of cosmic rays in different channels. FermiLAT has measured the photon flux from the Galactic Center and from Dwarf Spheroidal Galaxies, the latter have allowed to probe the canonical DM annihilation cross section for DM lighter than 40GeV [9]. Furthermore an anomaly corresponding to a gamma-ray line at 130 GeV has been extracted from the FermiLAT data [10, 11]. FermiLAT [12], PAMELA [13]

and AMS [14] have measured the positrons fluxes, showing an anomaly at high energies while PAMELA data on anti-protons are in perfect agreement with expectations from the background [15]. AMS will pursue the measurement of antimatter (positrons, antiprotons and antideuterons) and photon fluxes. Despite some anomalies, none of these searches lead to conclusive evidence for DM. Finally neutrino signals from annihilation of dark matter captured by the Sun are being probed by neutrino telescopes such as SuperK [16], ANTARES [17] or ICECUBE [18].

On a different front, the LHC has discovered the Higgs boson [19, 20] and has searched directly and indirectly - for example through their effect on B physics - for new particles that are predicted in extensions of the standard model with a DM candidate. Matching the properties of the Higgs particle imposes strong constraints on the parameter space of DM models. Furthermore the LHC is searching for DM signals in events where a pair of DM particles are produced in association with a jet or a photon [21, 22, 23], these searches provide the best limit on effective DM interactions with nucleons for light DM. Confronting the predictions from a variety of particle physics models which possess a stable weakly interacting massive particle (WIMP) with all these observations will help to corner the properties of a new cold dark matter candidate or show that one has to turn to other candidates that act rather as warm dark matter.

The interpretation of the abundant recent and upcoming data from these different types of experiments requires tools to compute accurately the various signals for DM interaction and this in the context of different particle physics models. `micrOMEGAs` is a code designed to predict dark matter signatures in various extensions of the SM which possess a discrete symmetry that guarantees the stability of the DM particle.<sup>1</sup> This code includes some of the common extensions of the SM : the minimal supersymmetric standard model (MSSM) and its extensions (NMSSM, CPVMSSM), the little Higgs model, the inert doublet model and incorporates various constraints from collider physics and precision measurements for some of these models. Furthermore the code can accommodate user defined models. In this new version we extend the functionalities of `micrOMEGAs` in three main directions:

- generalizing the Boltzmann equations to include asymmetric dark matter and semi-annihilations. The DM asymmetry is taken into account when computing direct/indirect detection rates.
- incorporating loop-induced decays of Higgs particles to two-photons and two-gluons, and computing the signal strength for Higgs production in various channels that can be compared to results from LHC searches. Limits on the Higgs sector can also be obtained through an interface to HiggsBounds
- adding a module for neutrino signature from DM capture in the Sun and the Earth

In addition the following improvements to the previous version are incorporated

- Annihilation cross sections for some selected 3-body processes in addition to the 2-body tree-level processes. The 3-body option can be included in the computation of the relic density and/or for annihilation of dark matter in the galaxy.

---

<sup>1</sup>DarkSUSY [24], Isared [25] and SuperIsorelic [26] are other public codes that compute the signatures of dark matter. These codes are confined to supersymmetric models.

- Possibility of using different tables for the effective degrees of freedom ( $g_{eff}(T), h_{eff}(T)$ ) in the early Universe
- Annihilation cross sections for the loop induced processes  $\gamma\gamma$  and  $\gamma Z^0$  in the NMSSM and the CPVMSSM
- New function for incorporating DM clumps
- New function to define the strange quark content of the nucleon
- The LanHEP [27] source code for new models is included
- New models with scalar DM are included (Inert doublet model [28] and model with  $Z_3$  symmetry [29])
- New implementation of the NMSSM which uses the Higgs self-couplings and the particle spectrum calculated in NMSSMTools\_4.0 [30, 31]
- New versions of spectrum generators used in the MSSM (Suspect\_2.4.1) [32] and in the CPVMSSM (CPsuperH2.3) [33]
- Extended routines for flavor physics in the MSSM
- New facilities to compute DM observables independently of the model
- Update in interface tools to read files produced by other codes, this allows easy interface to other codes

`micrOMEGAs3` contains all the routines available in previous versions although the format used to call some routines has been changed. In particular global variables are used to specify the input parameters of various routines. All functions of `micrOMEGAs` are described in the manual, `manual3.pdf`, to be found in the `man` directory, see also the lecture notes [34].

In this paper we first describe in section 2 the generalization of the relic density routine to include asymmetric dark matter and semi-annihilation processes as well as more general thermodynamics of the Universe. Section 3 describes the new module to compute the neutrino-induced muon flux from DM captured in the Sun or the Earth. In section 4, we give a brief description of improvements on the computation of the direct and indirect DM signals, in particular to take into account possible DM clumps. In section 5 we describe new facilities to compute more precisely the partial widths of the Higgs and incorporate LHC results on the Higgs. A brief description of SUSY models is provided in section 6. Section 7 contains a description of the functions that allow to work with external codes. Finally sample results are presented in Section 8.

## 2 Generalization of the relic density computation

The Boltzmann equation that describes the number density of DM that is used to solve for the abundance of DM today and obtain its relic density is based on several assumptions. First, it is assumed that the DM candidate is either a self-conjugate particle or that there is no DM anti-DM asymmetry, and that there exists a discrete symmetry such as R-parity

in supersymmetry that guarantees the stability of the lightest particle. Furthermore this symmetry permits only annihilation of pairs of DM particles into SM particles. Second, the annihilation cross section of DM particles is taken to be typically of electroweak strength such that DM particles are in thermal equilibrium in the early Universe and eventually freeze-out as the Universe cools down. Third, the contribution of the relativistic degrees of freedom to the entropy density and energy density of the Universe are taken to go as  $T^4$  and  $T^3$  respectively.

In the following we will modify some of these assumptions by introducing the possibility of asymmetric DM and of new annihilation processes called semi-annihilation where two DM particles annihilate into another DM particle and a SM particle. We will furthermore include the possibility of DM annihilation into 3-body processes. We will continue to assume that DM annihilation is typically of electroweak strength and keep the case of very weak interactions for further development. We will also postpone the full implementation of a modification of the entropy and energy contributions to the Universe for a further version but will discuss the possibility to modify the temperature dependence of the effective number of degrees of freedom.

## 2.1 Asymmetric dark matter

We consider a dark matter particle that is not self-conjugate, with the particle being  $\chi = \chi^+$  and the antiparticle  $\bar{\chi} = \chi^-$ . This occur for example when the DM particle is a Dirac fermion [35] or a complex scalar [36, 37]. The Boltzmann equations for the abundance of a DM particle –defined as the number density divided by the entropy density - have to be generalized [38, 39, 40]. Recall that for a self-conjugate DM particle,  $\chi$ ,

$$\frac{dY_\chi}{ds} = \frac{\langle \sigma v \rangle}{3H} (Y_\chi^2 - Y_{eq}^2) \quad (1)$$

where  $\langle \sigma v \rangle$  is the relativistic thermally averaged annihilation cross-section,  $Y_{eq}$  is the equilibrium abundance,  $s$  the entropy and  $H$  the Hubble constant.

We define  $Y^+$  and  $Y^-$  as the abundances of the DM particle/anti-particle ( $\chi/\bar{\chi}$ ). At very high temperature, we assume that an asymmetry has already taken place such that  $Y^+ \neq Y^-$  but that at later times the system is in equilibrium in a universe governed by a standard cosmology. We assume that annihilation to SM particles occurs only between  $\chi^+$  and  $\chi^-$  and not among same charge DM. This could be the result of some conserved global charge carried by the DM particles. One should therefore expect that the difference between the abundances  $Y^+$  and  $Y^-$  does not change during the thermal evolution. The evolution equation is then

$$\frac{dY^\pm}{ds} = \frac{1}{3H} (\langle \sigma v^{+-} \rangle (Y^+ Y^- - Y_{eq}^+ Y_{eq}^-)) \quad (2)$$

with  $Y_{eq}^+(T) = Y_{eq}^-(T) = 1/2 Y_{eq}(T)$  and  $\frac{1}{2} \langle \sigma v^{+-} \rangle = \frac{1}{2} \langle \sigma v^{-+} \rangle = \langle \sigma v \rangle$ .

Subtracting the two equations in Eq. 2 we obtain

$$\frac{dY^+}{ds} - \frac{dY^-}{ds} = 0 \quad (3)$$

implying that the difference of abundances

$$\Delta Y = Y^+ - Y^- \quad (4)$$

is constant as expected.

To proceed, we define the quantity  $Y \equiv 2\sqrt{Y^+Y^-}$  which is equivalent to the abundance  $Y = Y_\chi$  for a self-conjugate DM. Using the abundance for each species,

$$Y^\pm = \frac{\pm\Delta Y + \sqrt{Y^2 + \Delta Y^2}}{2} \quad (5)$$

the evolution equation for  $Y$  is derived

$$\begin{aligned} \frac{dY}{ds} &= \frac{\langle \sigma v \rangle}{3H} \frac{Y^+ + Y^-}{Y} (Y^2 - Y_{eq}^2) \\ &= \frac{\langle \sigma v \rangle}{3H} (Y^2 - Y_{eq}^2) \sqrt{1 + \left(\frac{\Delta Y}{Y}\right)^2} \end{aligned} \quad (6)$$

This equation is similar to the equation for a self-conjugate DM candidate save for an additional term. It can be solved numerically using the usual procedure [41], to obtain the abundances today,  $Y_0 = Y(T = T_0)$ . The total relic density of the DM particle/antiparticle is then given by

$$\Omega h^2 = \frac{8\pi}{3H_{100}^2} \frac{m_\chi}{M_{\text{Planck}}} \frac{\sqrt{Y_0^2 + \Delta Y^2}}{s_0} \quad (7)$$

where  $s_0$  is the entropy today,  $H_{100} = 100\text{km/s/Mpc}$  (the Hubble constant today is  $H_0 = H_{100}h$ ), and  $M_{\text{Planck}}$  is the Planck mass. The relic density of each specie can be expressed in terms of the asymmetry parameter  $\delta_{DM}$ ,

$$\Omega_\pm h^2 = \frac{\Omega h^2}{1 + e^{\mp\delta_{DM}}} \quad (8)$$

with

$$\delta_{DM} = \log \left( \frac{\sqrt{Y_0^2 + \Delta Y^2} + \Delta Y}{\sqrt{Y_0^2 + \Delta Y^2} - \Delta Y} \right). \quad (9)$$

Note that the asymmetry,  $\Delta Y$ , will always increase the relic abundance as compared to the one obtained in the same model but without an asymmetry.

To illustrate the impact of the asymmetry on the relic density, we use a simple extension of the SM with one extra lepton generation,  $e_4, \nu_4$  where  $\nu_4$  is a massive Dirac neutrino. These new leptons interact with SM gauge bosons but do not mix with the first three generations. We assume an ad-hoc discrete symmetry where only  $e_4, \nu_4$  have  $R = -1$  while SM particles have  $R = 1$ . Thus when  $\nu_4$  is lighter than  $e_4$  it is stable and a potential DM candidate. The dependence of  $\Omega h^2$  on  $\Delta Y$  for several DM masses is displayed in Fig. 1. <sup>2</sup> When  $\Delta Y$  is small there is no changes in the symmetric component and the asymmetry will lead to a small increase in the relic abundance. When the asymmetry times  $\sigma v$  is large,  $Y_-$  is very small and the relic density is determined by  $\Delta Y$ , this shows up as a linear dependence of the relic density with  $\Delta Y$  in Fig. 1. Note that since in this case one DM component has disappeared completely, a signal in indirect detection is

---

<sup>2</sup>This model is only illustrative and would need to include new quarks to be anomaly free, furthermore the light DM masses are incompatible with the bounds on the Higgs invisible width that can be obtained from LHC results [42, 43].

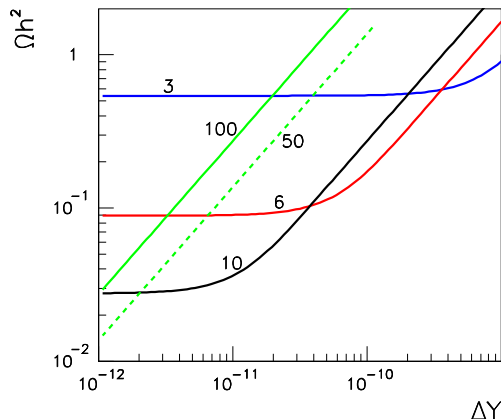


Figure 1:  $\Omega h^2$  as a function of  $\Delta Y$  for different DM masses in the 4th generation Dirac neutrino dark matter model for DM masses of 3, 6, 10, 50, 100 GeV as indicated.

not expected. The linear dependence starts at lower values of  $\Delta Y$  for larger DM masses, since in this model  $\sigma v$  also increases with the DM mass up to  $m_{DM} \approx 50$  GeV. Note that when finding the starting point for the solution of the evolution equation we assume that  $Y - Y_{eq} \gg Y_{eq}$ , when  $\Delta Y$  times  $\sigma v$  is very large this assumption will fail, this means that the freeze-out picture is inadequate. In this example  $\sigma v$  is strongly enhanced when  $m_{DM} \approx m_Z/2$  and our solution method breaks when  $\Delta Y \approx 10^{-10}$  for this mass.

In `micrOMEGAs` the asymmetry  $\Delta Y$  is a global parameter, `deltaY`, that can be set anywhere in the code. The relic density computation takes it into account automatically to obtain both  $\Omega h^2$  and  $\delta_{DM}$ , Eq. 9. The latter is also a global parameter `DMasymm`, see Table (2). Furthermore the parameter `DMasymm` will have a direct impact on other observables computed in `micrOMEGAs`.

The computation of the rate for dark matter scattering on nuclei is normally done averaging the cross section for DM and anti-DM scattering on nucleons and depends on the local DM density which is the sum of DM ( $\rho_\chi$ ) and anti-DM ( $\rho_{\bar{\chi}}$ ) density. When the asymmetry parameter  $\delta_{DM}$  is non-zero, the rate will take into account the relative abundance of matter and anti-matter given the value of the local DM density specified as a global parameter. For indirect detection, the production rate of particles from DM annihilation is also modified to take into account the density of DM and anti-DM,

$$Q = \frac{1}{2} \langle \sigma v \rangle \frac{\rho_\chi \rho_{\bar{\chi}}}{m_\chi^2} \frac{dN_a}{dE}, \quad (10)$$

and the local density is  $\rho_\chi + \rho_{\bar{\chi}}$ . Note that the parameter `DMasymm`= $\delta_{DM}$ , which characterizes the asymmetry between the relic density of the two components, is also a global parameter. If reset after the relic density computation, it will be taken into account for computing direct and indirect detection rates and thus will allow the user to examine the impact of an asymmetry on these observables.

## 2.2 Semi-annihilation

With discrete symmetries larger than  $Z_2$ , one introduces new DM annihilation processes as well as the possibility of having more than one DM candidate corresponding to the lightest particle of two distinct dark sectors. Although `micrOMEGAs` has been modified to include more than one DM candidate [29], this possibility has been implemented only within the context of some specific DM models and is not included in this public distribution. In this section we therefore discuss only the impact of new processes of the type  $\chi\chi \rightarrow \bar{\chi}X$  where  $\chi$  is any particle from the dark sector ( $\bar{\chi}$  correspond to anti-particles) and  $X$  is any SM particle. These processes are called *semi-annihilation* [44, 45, 29]

The simplest example of a discrete symmetry which leads to semi-annihilation processes is  $Z_3$ . The SM particles have  $Z_3$  charge 0, while particles (anti-particles) in the dark sector have  $Z_3$  charges 1 and  $-1$  respectively. Hence such models feature as usual only one DM candidate. With semi-annihilations, the equation for the number density reads

$$\frac{dn}{dt} = -\langle v\sigma^{\chi\bar{\chi}\rightarrow XX} \rangle (n^2 - n_{\text{eq}}^2) - \frac{1}{2}\langle v\sigma^{\chi\chi\rightarrow\bar{\chi}X} \rangle (n^2 - n n_{\text{eq}}) - 3Hn. \quad (11)$$

We define

$$\sigma_v \equiv \langle v\sigma^{\chi\bar{\chi}\rightarrow XX} \rangle + \frac{1}{2}\langle v\sigma^{\chi\chi\rightarrow\bar{\chi}X} \rangle \quad \text{and} \quad \alpha = \frac{1}{2} \frac{\langle v\sigma^{\chi\chi\rightarrow\bar{\chi}X} \rangle}{\sigma_v}, \quad (12)$$

which means that  $0 \leq \alpha \leq 1$ . In terms of the abundance,  $Y = n/s$ , where  $s$  is the entropy density, we obtain

$$\frac{dY}{dt} = -s\sigma_v (Y^2 - \alpha Y Y_{\text{eq}} - (1 - \alpha) Y_{\text{eq}}^2) \quad (13)$$

or

$$3H \frac{dY}{ds} = \sigma_v (Y^2 - \alpha Y Y_{\text{eq}} - (1 - \alpha) Y_{\text{eq}}^2). \quad (14)$$

To solve this equation we follow the usual procedure [41]. Writing  $Y = Y_{\text{eq}} + \delta Y$  we find the starting point for the numerical solution of this equation with the Runge-Kutta method using

$$3H \frac{dY_{\text{eq}}}{ds} = \sigma_v Y_{\text{eq}} \delta Y (2 - \alpha), \quad (15)$$

where  $\delta Y \ll Y$ . This is similar to the standard case except that  $\delta Y \rightarrow \delta Y(1 - \alpha/2)$ . Furthermore, when solving numerically the evolution equation, the decoupling condition  $Y^2 \gg Y_{\text{eq}}^2$  is modified to

$$Y^2 \gg \alpha Y Y_{\text{eq}} + (1 - \alpha) Y_{\text{eq}}^2. \quad (16)$$

This implies that the freeze-out starts at an earlier time and lasts until a later time as compared with the standard case. Although semi-annihilation processes can play a significant role in the computation of the relic density, the solution for the abundance depends only weakly on the parameter  $\alpha$ , typically only by a few percent. This means in particular that the standard freeze-out approximation works with a good precision. Explicit examples of the impact of semi-annihilation can be found in [29, 37]. The function `onechannel` (see section 2.5) can be used to obtain the contribution of each semi-annihilation channel and from there extract  $\alpha$ .

There is no special need to indicate to `micrOMEGAs` that a model contains semi-annihilation processes, as long as all particles in the dark sector are properly identified, `micrOMEGAs` will find the relevant processes. Note that the modified Boltzmann equation

including both asymmetric DM and semi-annihilation is implemented in the code, however both terms cannot be present simultaneously in a specific model.

## 2.3 Thermodynamics of the Universe

The formulas that give the contribution of one relativistic degree of freedom to the entropy density and energy density of the Universe are rather simple. For bosons,

$$\rho_b = \frac{\pi^2}{30}T^4, \quad s_b = \frac{2\pi^2}{45}T^3 \quad (17)$$

while the corresponding functions for fermions have an additional factor  $\frac{7}{8}$ . In the generic case one can write

$$\rho(T) = \frac{\pi^2}{30}T^4 g_{eff}(T), \quad s(T) = \frac{2\pi^2}{45}T^3 h_{eff}(T) \quad (18)$$

where  $g_{eff}(T)/h_{eff}(T)$  count the effective numbers of degrees of freedom.<sup>3</sup> At freeze-out temperatures, the contribution of DM should be strongly suppressed, only SM particles contribute to  $g_{eff}$  and  $h_{eff}$ .<sup>4</sup> At low temperature ( $T \ll 100MeV$ ), the effective number of degree of freedom is defined by photons, neutrinos, light leptons. As the temperature increases, one has to add the quarks degrees of freedom. There is a problem of correct matching between the low and high temperature region.

This issue was studied in [46] where other functions which feature different matching between the two regions have been derived. By default `micrOMEGAs` uses the tabulated functions for  $g_{eff}(T)/h_{eff}(T)$  obtained in [47, 48], these tables assume that  $T_{QCD} = 150MeV$ . The temperature dependence of  $h_{eff}$  is displayed in Fig. 2.

The tabulated functions of [46] are also available.  $h_{eff}(T)$  for three of those functions, B, B2 and B3, are compared to the default function in Fig. 2, numerically the difference is small. A function (`loadHeffGeff`) allows to substitute any table, see section 2.5. The different functions for  $h_{eff}$  can induce a shift in the value of the relic density, typically of a few percent. The larger shifts are expected for light DM masses, especially for those where the freeze-out temperature is near the QCD transition region (that is  $T_{fo} \approx m_{DM}/25 \approx 150MeV$ ). As an example, we consider the MSSM and display in Fig. 2 the resulting shift in  $\Omega h^2$  for different choices of  $h_{eff}(T)$  as a function of the neutralino mass. The neutralino mass is varied by changing  $M_1$  while keeping  $M_{r3} = M_1 + 51GeV$ , for each point the value of  $\mu$  is adjusted such that  $\Omega h^2 \approx 0.1147$  [49]. Other MSSM soft parameters are fixed to  $M_2 = 400GeV$ ,  $M_3 = 1.8TeV$ ,  $M_{Li} = M_{Ri} = 500GeV$ ,  $M_{Qi} = 2TeV$ ,  $M_{ui} = M_{di} = 1.5TeV$ ,  $A_t = A_b = -2.8TeV$ ,  $M_A = 700GeV$ ,  $\tan \beta = 35$ .

## 2.4 Three-body processes

The pair annihilation of DM particles into a pair of SM particles may not be allowed for some kinematic and/or symmetry reasons. A known example is the suppression of the s-wave production of massless fermions in the case of a Majorana DM. This suppression is

---

<sup>3</sup> $g_{eff}(T)$  and  $h_{eff}(T)$  are related via the condition  $\frac{d\rho(T)}{dT} = T \frac{ds(T)}{dT}$

<sup>4</sup>We assume that at low temperatures when DM contributes significantly to the matter density, the formation of DM has been completed and  $Y(T) = \text{Const}$ .

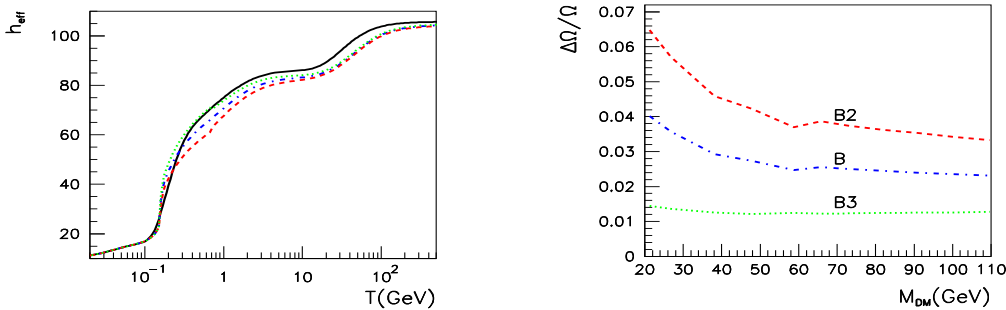


Figure 2: Left panel : Values of  $h_{eff}$  as a function of  $T$  for different QCD equation of states, corresponding to the default `micrOMEGAs` table with  $T_{QCD} = 150\text{MeV}$  (black/full), and to case B (blue/dot-dash), B2(red/dash), B3(dot/green) of Ref. [46]. Right panel : Relative difference between  $\Omega h^2$  computed with the default table for  $h_{eff}$  and cases B,B2,B3, same color code as left panel.

lifted by the emission of photons in association with the fermion pair. Another example to which we now turn is the case where annihilation into gauge bosons is kinematically suppressed. The cross section for annihilation into off-shell  $W$ 's can then be as large as that of other 2 body annihilation channels. This effect was shown to be particularly important in models such as the inert doublet model where the DM candidate is a scalar and has a standard  $SU(2)$  coupling to  $W$ 's [50, 52, 51].

`micrOMEGAs` has a switch that allows to include three and four-body final states involving one/two off-shell gauge boson ( $W/Z$ ). A similar procedure is also used for the decay of a Higgs into 3/4-body final states. For DM annihilation or co-annihilation, we consider processes such as

$$\chi\chi' \rightarrow XV \quad (19)$$

where  $V = W, Z$ . To take into account the process with an off-shell  $V$ , we use CalcHEP to compute the 3-body process

$$\chi\chi' \rightarrow Xll' \quad (20)$$

where  $ll'$  is one leptonic decay channel of  $V$ . To obtain the total annihilation cross section into a virtual  $V$ , we divide this result by the branching ratio,  $Br(V \rightarrow ll')$ . In general for  $l, l'$  we use leptons of the first generation except when  $X$  is a first generation lepton (this can happen in some co-annihilation processes). In this case we use second generation leptons to avoid additional poles in matrix elements from unwanted diagrams that do not contain a virtual  $V$ . For processes involving a virtual  $Z$  we use  $ll' = \nu\bar{\nu}$  to avoid extra diagrams with virtual photons, even though those are expected to be small due to the large virtuality of the photon.

Processes with three-body final states can contain diagrams that do not involve a virtual  $V$ , our procedure for reconstructing the total 3-body cross section from only one specific final state would in this case be spoiled. Ideally we would need to select only the diagrams with a virtual  $V$  corresponding to the process in Eq. 19; this however can induce breaking of  $SU(2)$  gauge invariance. To solve this problem we select diagrams

where the total number of virtual vector bosons (W and Z) is at least 1, thus ensuring a gauge invariant set of diagrams.

If  $X$  is also a SM vector boson then the procedure we have just described does not work very well since one or both of the  $V$  can be off-shell. First, note that far below the threshold for  $VV$  production, the total cross section is twice the one for  $Vll'$  since each vector boson can be off-shell, while very near threshold the 3-body result should be close to the 2-body result. We therefore need to compute the cross section for four-body final states. This is however computer-time consuming and would significantly slow down our code to a point where large scans of parameter space cannot be realized. We therefore use a trick to evaluate the 4-body process from the 3-body result after applying a K-factor. To obtain the K factor we assume that the 4-body matrix element is proportional to

$$M_{4\text{-body}} \propto \frac{\left[ (m_1 m_2)^2 + \frac{1}{8} (s - m_2^2 - m_1^2)^2 \right]}{\frac{\Gamma_1}{((m_1^2 - m_1'^2)^2 - \Gamma_1^2 m_1'^2)} \frac{\Gamma_2}{((m_2^2 - m_2'^2)^2 - \Gamma_2^2 m_2'^2)}} \quad (21)$$

where  $m_1, m_2$  are virtual masses and  $m_1', m_2'$  are pole masses,  $\Gamma_1, \Gamma_2$  are particle widths and  $s = 4m_\chi^2$ . Note that this is the form of the matrix element for Higgs decay into 4-body final state through two virtual gauge bosons. We integrate this matrix element with  $\Gamma_1 = 0$  in order to simulate the 3-body result, then we integrate the same matrix element with the correct value for  $\Gamma_1$ . The ratio of these integrals gives the K factor. We have compared the value of the annihilation cross section at freeze-out obtained using the K-factor with the one obtained with the complete 4-body kinematics, in the MSSM for the benchmark point described below the difference is less than 5%.

We consider only the contribution from virtual W's and Z's. The contribution from a virtual Higgs is expected to be small because the width is very small. Contributions from virtual top quarks could also be important for DM masses below the top threshold [50], such contributions will be included in a future upgrade.

In Fig. 3 we compare the DM relic density computed using 3-body final state with the one using only 2-body final states. In the MSSM, the LSP mass is changed by varying  $M_1$ , other soft parameters are fixed to  $M_2 = 200\text{GeV}$ ,  $M_3 = 1\text{TeV}$ ,  $\mu = 126\text{GeV}$ ,  $M_A = 1\text{TeV}$ ,  $\tan\beta = 10$ ,  $M_{Li} = M_{Ri} = M_{Qi} = M_{ui} = M_{di} = 1.5\text{TeV}$ ,  $A_t = 2.8\text{TeV}$ . Differences up to 17% are found for masses just below the W-pair production. Furthermore differences up to 10% are also found for LSP masses below  $m_h/2$ . Note however that in this example the relic density is very small for masses below  $m_h/2$  since the Higgs exchange in s-channel gives an important contribution to DM annihilation. In the IDM, we take  $\lambda_L = \lambda_2 = 0.01$ ,  $m_h = 125\text{GeV}$ , and vary the DM mass imposing  $m_A - m_{DM} = m_{H^+} - m_{DM} = 50\text{GeV}$ . For DM masses heavier than  $m_h/2$  the difference between the 2-body approximation and the calculation that includes off-shell W/Z's can reach one order of magnitude, as was shown in Ref. [52]. For DM masses below  $m_h/2$  where annihilation is completely dominated by Higgs exchange, we find basically the same result for the 2-body and 3-body final states, even though the Higgs width is quite different in the two cases. This is because the annihilation cross section does not depend on the value of the Higgs width as long as the Higgs width and the DM pair annihilation are computed with the same approximation. Recall that in `micrOMEGAs` the two-body option does not include the off-shell boson final states in the Higgs width, this explains the difference with the results in Ref. [52].

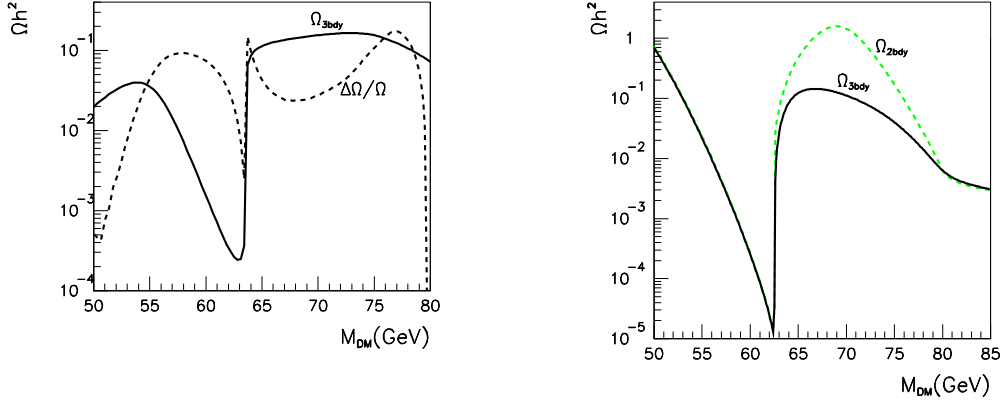


Figure 3: Left panel :  $\Omega h^2$  as a function of  $M_{DM}$  in the MSSM (full) and relative difference between the 3-body and 2-body value (dash). The soft parameters used are specified in the text. Right panel :  $\Omega h^2$  as a function of  $M_{DM}$  in the IDM including the 3-body final states (full) and only 2-body final states (dash).

## 2.5 New functions and switches

As in previous versions, the relic density computation is performed with the function `darkOmega` as described in [53], new features include the 3-body final state, which can be taken into account by specifying

- `VWdecay, VZdecay`

Switches to turn on/off processes with off-shell gauge bosons in final states for DM annihilation and particle decays. If `VW/VZdecay=1`, the 3-body final states will be computed for annihilation processes only while if `VW/VZdecay=2` they will be included in coannihilation processes as well. By default the switches are set to (`VW/VZdecay=0`).<sup>5</sup> Note that `micrOMEGAs` calculates the width of each particle only once. A second call to the function `pWidth` (whether an explicit call or within the computation of a cross section) will return the same result even if the user has changed the `VW/VZdecay` switch. To clean the decay table and re-activate the `VW/VZdecay` switches, one has to call

- `clearDecayTable()`

to force `micrOMEGAs` to recalculate particle widths according to the new value of `VW/VZdecay`. The `sortOddParticles` command which must be used to recompute the particle spectrum after changing the model parameters also cleans the decay table.

If particle widths were stored in the SLHA file downloaded by `micrOMEGAs`, then the SLHA value will be used by `micrOMEGAs`. To prevent downloading of decays one can download SLHA file using `slhaRead(fileName, mode=4)`, see description in Section 7.

Two new global parameters are available to set the DM asymmetry:

- `deltaY`

describes the difference between the DM and anti-DM abundances, Eq. 4.

- `DMasymm`

is the relic density asymmetry parameter in Eq. (9) and is evaluated by `micrOMEGAs` while calculating the relic density with an initial asymmetry `deltaY`. This parameter can also

<sup>5</sup>Including the 3-body final states can significantly increase the execution time for the relic density.

be reset after the relic density computation and will be taken into account for direct and indirect detection rates.

The temperature dependence of the effective number of degrees of freedom can be set with

- `loadHeffGeff(char*fname)`

loads the file `fname` which contains a table of  $h_{eff}(T), g_{eff}(T)$ . A positive return value corresponds to the number of lines in the table. A negative return value indicates the line which creates a problem (e.g. wrong format), the routine returns zero when the file `fname` cannot be opened. Several files containing tables of  $h_{eff}(T), g_{eff}(T)$  are stored in the directory `sources/data`. The default file is `std_thg.tab` [47, 48] and is downloaded automatically if `loadHeffGeff` is not called by the user. Five other files `HP_X_thg.tab` where  $X = \{A, B, B2, B3, C\}$  contain data sets from [46]. The user can substitute his/her own table as well, if so, the file must contain three columns containing the numerical values for  $T, h_{eff}, g_{eff}$ , the data file can also contain comments on lines starting with `#`.

Several new functions that give information on the contribution of different channels to DM annihilation have been added in this version

- `vSigma(T, Beps, fast)`

calculates the thermally averaged cross section for DM annihilation times velocity at a temperature  $T$  [GeV], see Eq.2.6 in [54]. The value for  $\sigma v$  is expressed in [pb]. The parameter `Beps` defines the criteria for including coannihilation channels. The `fast=1/0` option switches between the *fast/accurate* calculation. The global array `vSigmaTCh` contains the contribution of different channels to `vSigma`. `vSigmaTCh[i].weight` specifies the relative weight of the  $i^{th}$  channel

`vSigmaTCh[i].prtcl[j]` ( $j=0, 4$ ) define particles names for the  $i^{th}$  channel.

The last record in `vSigmaTCh` array has zero weight and NULL particle names. In the Fortran version, the function `vSigmaTCh(i,weight,particles)` with  $i \geq 1$ , serves the same purpose. This function returns 0 if  $i$  exceeds the number of annihilation channels and 1 otherwise. *real\*8 weight* gives the relative contribution of each annihilation channel. *character\*10 particles(4)* contains the names of particles in the annihilation process.

- `oneChannel(Xf, Beps, p1, p2, p3, p4)`

calculates the relative contribution of the channel  $p1, p2 \rightarrow p3, p4$  to  $(\Omega h^2)^{-1}$  where  $p1, \dots, p4$  are particle names. To make a summation over several channels one can substitute "\*" instead of the particle name.

- `omegaCh`

is an array that contains the relative contribution and particle names for each annihilation channel. In the Fortran version one uses instead the function

`omegaCh(i,weight,particles)`. These arrays are similar to `vSigmaTCh` described above. The array `omegaCh` is filled after calling either `darkOmegaF0` or `printChannels`.

### 3 DM in neutrino telescopes

After being captured, DM particles concentrate in the center of the Sun/Earth and then annihilate into Standard Model particles. These SM particles further decay producing neutrinos that can be observed at the Earth. Annihilation of DM particles in the galaxy is also a source of neutrinos. As for other indirect searches, the shape of the neutrino flux

depends on the dominant DM annihilation channel into SM particles. Direct annihilation of DM into neutrinos gives the hardest spectrum followed by muons and W's. As we will see below the signal for neutrinos coming from DM captured in a celestial body is essentially determined by the cross section for DM scattering on nuclei and is thus related to direct detection searches while galactic neutrinos probe the DM annihilation cross section.

The neutrino signal from DM captured in the Sun or Earth usually dominates over the one originating from DM annihilation in the galaxies. The best limit on galactic neutrinos have been achieved by IceCUBE [55], however the limit on the DM annihilation cross section are still orders of magnitudes above the canonical cross section required to achieve the relic density assuming a standard cosmological scenario. Limits on the muon flux from neutrinos captured in the Sun were obtained by Super-Kamiokande, [16], Baksan [56], Amanda and ICECUBE [18], and are currently more sensitive than direct detection experiments in probing DM nuclei spin dependent cross sections on protons. The best limit on the SD cross section on protons is currently obtained by ICECUBE,  $\sigma^{SD} = 1.2 \times 10^{-40} \text{cm}^{-2}$  for  $m_{DM} = 200 \text{GeV}$  [18]. Note that ICECUBE with the DeepCore extension has a threshold energy of 10GeV [57] while Super-Kamiokande has a threshold of 1.6 GeV and is thus the best detector for light DM candidates. The neutrino flux and the induced muon flux from DM captured in the Sun and the Earth is a new module and will be described below.

### 3.1 Capture rate

The capture rate for DM particles in the core of the Sun/Earth depends on the DM-nucleus scattering cross-section, as well as on the DM velocity distribution and local density. A DM particle will get captured if after scattering with a nucleus at a distance  $r$  from the center, its velocity is lower than the escape velocity,  $v_{esc}(r)$ , defined via gravitational potential

$$\frac{v_{esc}(r)^2}{2} = \phi(r) \quad (22)$$

The capture rate was derived in [58]

$$C_\chi = \frac{\rho_\chi}{m_\chi} \int_0^\infty du f(u) \int 4\pi r^2 dr \sum_A \sigma_{\chi A} n_A(r) \frac{\beta_A}{\alpha_A} \theta(e^{-\alpha_A u^2} - e^{-\alpha_A(u^2 + v_{esc}^2(r))/\beta_A}) \quad (23)$$

where  $u$  is the WIMP velocity at infinity,  $f(u)$  is the WIMP velocity distribution normalized by the condition

$$\int_0^\infty u f(u) du = 1 \quad (24)$$

$\sigma_{\chi A}$  is the scattering cross section for DM on nuclei,  $n_A$  is the number density of nucleus A, and

$$\alpha_A = \frac{1}{3} m_\chi m_A R_A^2, \quad \beta_A = \frac{(m_\chi + m_A)^2}{4m_\chi m_A} \quad (25)$$

where  $m_A$  is the mass and  $R_A$  the radius of nucleus A, The computation of  $\sigma_{\chi A}$  takes into account the fact that the WIMP scattering cross section is velocity dependent which implies a form factor dependence

$$|F(q^2)|^2 = \exp\left(\frac{-q^2 R_A^2}{3}\right) \quad (26)$$

where  $q$  is the momentum transfer. For the Gaussian form factor<sup>6</sup> we assume that

$$R_A = (0.91(m_A/\text{GeV})^{1/3} + 0.3) \times 10^{-13} \text{cm} \quad (27)$$

For spin-independent interactions which add coherently, the sum is performed over all nuclei up to <sup>59</sup>Ni. For spin-dependent interaction, there is no coherence effect  $\propto A^2$ , therefore hydrogen gives the largest contribution, in this case we do not include the form factor. The capture rate can be modified by finite temperature effects, however this effect is below 1% [58] so we neglect it. To calculate  $n_A(r)$  we use the profiles given [59] and [60].

### 3.2 Annihilation

When the DM is self-conjugated, the annihilation rate of captured particles is  $N_\chi^2 A_{\chi\chi}$  where  $N_\chi$  is the number of DM particles and

$$A_{\chi\chi} = \frac{\langle\sigma v\rangle_{\chi\chi}}{V_{eff}} \quad , \quad (28)$$

$V_{eff}$  is the effective volume of DM in the Sun/Earth. Assuming a Boltzmann thermal distribution of DM captured by the Sun/Earth one can get

$$V_{eff} = \left(4\pi \int_0^R r^2 dr e^{-\frac{\phi(r)m_\chi}{T_\chi}}\right)^2 / \left(4\pi \int_0^R r^2 dr e^{-2\frac{\phi(r)m_\chi}{T_\chi}}\right) \quad (29)$$

and  $\phi(r)$  is the gravitational potential. The WIMPs are trapped close to the center of the Sun, in this region we can consider that the temperature and the density are constant. We choose  $T_\chi = T(\bar{r})$  where  $\bar{r}$  is the mean radius of the WIMP distribution

$$\bar{r} = \left(\frac{6T(\bar{r})}{\pi^2 G \rho(\bar{r}) m_\chi}\right)^{1/2} \quad (30)$$

with  $G$  the Newton's constant. The mean radius can be solved numerically from the temperature and density profile of the Sun/Earth.

When DM is not self-conjugated, an additional term  $N_\chi N_{\bar{\chi}} A_{\chi\bar{\chi}}$  contributes to the DM annihilation rate where

$$A_{\chi\bar{\chi}} = \frac{\langle\sigma v\rangle_{\chi\bar{\chi}}}{V_{eff}} \quad (31)$$

### 3.3 Evaporation

DM captured in the Sun/Earth can scatter with nuclei inside the Sun/Earth and gain enough energy to escape from the Sun/Earth. Evaporation depends very sensitively on the DM mass, it is important for light DM. This effect was estimated in [62, 61], approximate formulas for the evaporation rate were derived in [63]. The evaporation rate [63]

$$E_\odot = \frac{8\sigma_c}{\pi^3 \bar{r}^3} \bar{v} \frac{m_\chi \phi(\bar{r})}{T(\bar{r})} e^{-m_\chi \phi(\bar{r})/T(\bar{r})} \quad (32)$$

---

<sup>6</sup>Note that in the direct detection module we use a Woods Saxon form factor rather than a Gaussian form factor as it is more accurate especially at large  $q^2$ , however the Gaussian form factor can be integrated analytically.

where  $\bar{r}$  is the mean radius (Eq. 30) and  $\bar{v}$  the mean speed of DM,

$$\bar{v} = \left( \frac{8T(\bar{r})}{\pi m_\chi} \right)^{1/2} \quad (33)$$

$T(r)$  is the temperature profile of the Sun/Earth. The evaporation rate depends also on the integrated scattering cross section of DM on nuclei inside a radius  $r_c$ ,  $\sigma_c$ ,

$$\sigma_c = \int_0^{r_c} \sum_A \sigma_{\chi A} n_A 4\pi r^2 dr \quad (34)$$

where  $r_c$  is taken to be the radius where the temperature drops to 95% of its value,  $T(r_c) = 0.95T(\bar{r})$ . Typically, evaporation in the Sun affects significantly DM particles lighter than 3 GeV and is irrelevant for heavier DM particles.

### 3.4 Neutrino flux

When the DM is self-conjugate, the equation describing the evolution of the number of DM particles  $N_\chi$  is simply

$$\dot{N}_\chi = C_\chi - A_{\chi\chi} N_\chi^2 - E_\chi N_\chi, \quad (35)$$

where the capture rate, the annihilation rate and the evaporation rate were given above, Eqs. 23,28,32. When the evaporation is negligible and the capture and annihilation rates are sufficiently large, equilibrium is reached and the annihilation rate is only determined by the capture rate.

$$\Gamma_{\chi\chi} = \frac{1}{2} A_{\chi\chi} N_\chi^2 = \frac{C_\chi}{2}. \quad (36)$$

The condition for equilibrium is  $\sqrt{C_\chi A_{\chi\chi}} t \gg 1$ . For the Sun, where  $t_\odot = 4.57 \times 10^9$  yrs, equilibrium is easily reached, for the Earth, equilibrium might not be reached. To take into account the most general case, we do not make assumptions about equilibrium and solve Eq. 35 numerically.

In models where the DM is not self-conjugate, one can get different capture rates for particles and antiparticles. Furthermore both particle–particle (antiparticle–antiparticle) and particle–antiparticle annihilation channels exist. For example for a Dirac fermion DM one can get  $\chi\chi \rightarrow \nu\nu$  ( $A_{\chi\chi}$ ) and  $\chi\bar{\chi} \rightarrow X\bar{X}$  ( $A_{\chi\bar{\chi}}$ ) where  $X$  is any SM particle. The equations describing the evolution of the number of DM (anti-)particles,  $N_\chi(N_{\bar{\chi}})$ , are then

$$\begin{aligned} \dot{N}_\chi &= C_\chi - A_{\chi\chi} N_\chi^2 - A_{\chi\bar{\chi}} N_\chi N_{\bar{\chi}} - E N_\chi, \\ \dot{N}_{\bar{\chi}} &= C_{\bar{\chi}} - A_{\chi\bar{\chi}} N_\chi N_{\bar{\chi}} - A_{\bar{\chi}\bar{\chi}} N_{\bar{\chi}}^2 - E N_{\bar{\chi}}, \end{aligned} \quad (37)$$

The capture and annihilation rates can be evaluated as above, and the two coupled equations solved numerically to extract the number density of DM and anti-DM. In the case that evaporation is negligible and equilibrium is reached, these equations can be solved analytically, see Appendix B.

After solving for the number density, one can compute the neutrino flux at the Earth. First define,

$$\Gamma_{\chi\chi} = \frac{1}{2} A_{\chi\chi} N_\chi^2; \quad \Gamma_{\bar{\chi}\bar{\chi}} = \frac{1}{2} A_{\bar{\chi}\bar{\chi}} N_{\bar{\chi}}^2; \quad \Gamma_{\chi\bar{\chi}} = A_{\chi\bar{\chi}} N_\chi N_{\bar{\chi}} \quad (38)$$

The total neutrino spectrum at the Earth, assuming self-annihilation channels are solely into neutrino pairs, is given by

$$\begin{aligned}\frac{d\phi_\nu}{dE_\nu} &= \frac{1}{4\pi d^2} \left( \Gamma_{\chi\chi} Br_{\nu\nu} \frac{dN_{\nu\nu}}{dE} + \Gamma_{\chi\bar{\chi}} \sum_f Br_{f\bar{f}} \frac{dN_f}{dE} \right), \\ \frac{d\phi_{\bar{\nu}}}{dE_{\bar{\nu}}} &= \frac{1}{4\pi d^2} \left( \Gamma_{\bar{\chi}\bar{\chi}} Br_{\bar{\nu}\bar{\nu}} \frac{dN_{\bar{\nu}\bar{\nu}}}{dE} + \Gamma_{\bar{\chi}\chi} \sum_f Br_{f\bar{f}} \frac{dN_f}{dE} \right),\end{aligned}\quad (39)$$

where  $d = d_\odot = 1.5 \times 10^8$  km for the Sun and  $d = d_\oplus = 6.378$  km for the Earth,  $Br_{\nu\nu}$  is the branching fraction for annihilation into neutrino pairs,  $Br_{f\bar{f}}$  the branching fraction into each particle/antiparticle final state  $f\bar{f}$ .  $N_f$  and  $N_{\nu\nu}(N_{\bar{\nu}\bar{\nu}})$  are the neutrino spectra resulting from those annihilations. The neutrino spectra originating from different annihilation channels into SM particles and taking into account oscillations and Sun/Earth medium effects were computed in [64], we use the tables given there. Note that for the neutrino pair production an average over the three flavors in the annihilation process is assumed. In models where light DM annihilate directly into neutrinos of a given flavor (e.g. the light sneutrino scenario in [65]) this is not the case, however this is still a good approximation since almost perfect 3-generation mixing is expected for neutrinos below 10 GeV propagating in the Sun [64].

### 3.5 Muon fluxes

Neutrinos that reach the Earth interact with rock below or water/ice within the detector and will give muons. To compare with the data, one must therefore compute the muon flux. First consider muons that are created inside the detector, leading to the contained muon flux, [66]

$$\frac{d\phi_\mu}{dE_\mu} = \rho_M N_A \int_{E_\mu}^{m_\chi} dE_\nu \frac{d\phi_\nu}{dE_\nu} \frac{d\sigma_{cc}(E_\nu)}{dE_\mu} \quad (40)$$

where  $\rho_M$  is the water density,  $N_A$  the Avogadro number, and  $\sigma_{cc}$  the cross section for charged current interactions for neutrinos on nucleons,  $\nu N \rightarrow \mu N'$ . This cross section is averaged over protons and neutrons.

When neutrinos interact with matter outside the detector, one must also take into account the fact that muons lose energy on their way to the detector. The energy loss for a muon is assumed to be

$$\frac{dE_\mu}{dz} = -\rho_M(\alpha + \beta E_\mu) \quad (41)$$

where  $\rho_M = 2.6$  g/cm<sup>3</sup> is the rock density and  $\alpha = 2 \times 10^{-3}$  GeV cm<sup>2</sup>/g,  $\beta = 3 \times 10^{-6}$  cm<sup>2</sup>/g characterize the average energy loss of the muon traveling through rock or water. A muon of energy  $E'_\mu$  will, after propagating a distance  $z$  have an energy  $E_\mu$ , where

$$E'_\mu = e^{\beta\rho z} \left( E_\mu + \frac{\alpha}{\beta} \right) - \frac{\alpha}{\beta} \quad (42)$$

and its survival probability will be

$$P_{surv}(E'_\mu, E_\mu) = \left( \frac{E_\mu}{E'_\mu} \right)^y \left( \frac{\alpha + \beta E'_\mu}{\alpha + \beta E_\mu} \right)^y \quad (43)$$

where  $y = m_\mu/(c\tau\alpha\rho_M)$  and  $\tau$  is the muon lifetime.

The upward muon flux is then [66]

$$\frac{d\phi_\mu}{dE_\mu} = \rho_M N_A \int_{E_\mu}^{m_\chi} dE_\nu \frac{d\phi_\nu}{dE_\nu} \int_0^{z_{max}} dz \frac{d\sigma_{cc}(E_\nu)}{dE'_\mu} e^{z\beta\rho} P_{surv}(E'_\mu, E_\mu) \quad (44)$$

where

$$z_{max} = \frac{1}{\beta\rho_M} \log \left( \frac{\alpha + E_\nu\beta}{\alpha + E_\mu\beta} \right) \quad (45)$$

Note that  $E'_\mu(z = z_{max}) = E_\nu$ .

The event rate takes into account the effective area of the detector. For Super-K, the detector is cylindrical with a radius  $R = 18.9$  m and a height 36.2 m. The muons that are stopped in the first 7 m are not observed, this corresponds to the muon energy threshold of  $E = 1.6$  GeV. Furthermore, only muons of energy larger than 7.7 GeV go through the detector. This means that for models with DM masses below 8 GeV, almost all the muons will be stopped within the detector.

Because of oscillations, the neutrino flux at the Earth will contain an almost equal mixture of electron, muon and tau neutrinos. Muon neutrinos will convert into muons detectable in a detector while electron neutrinos will produce electrons which will not propagate for very long. Finally tau neutrinos will produce taus which rapidly decay, one of the tau decay modes involves muons and will therefore induce a correction to the  $\nu_\mu$ -induced muon flux. We do not take this effect into account.

### 3.6 Functions for neutrino flux

- `neutrinoFlux(f,forSun,nu, nu_bar)`

calculates the muon neutrino/anti-neutrino fluxes near the surface of the Earth. This function a) calculates capture, annihilation, and evaporation rates, Eqs. 23,28,32; b) solves numerically Eq. 35 or Eq. 37; c) calculates all branchings of DM annihilation and substitute them in Eq. 39 to get the fluxes.

Here  $\mathbf{f}(\mathbf{v})$  is the DM velocity distribution normalized as in Eq. 24. The units are  $km/s$  for  $\mathbf{v}$  and  $s^2/km^2$  for  $\mathbf{f}(\mathbf{v})$ . At first approximation, one can use the same `Maxwell` function introduced for direct detection. If `forSun==0` then the flux of neutrinos from the Earth is calculated, otherwise this function computes the flux of neutrinos from the Sun as described in section 3.1. The calculated fluxes are stored in `nu` and `nu_bar` arrays of dimension `NZ=250`. The neutrino fluxes are expressed in `[1/Year/km2]`. The function `SpectdNdE(E,nu)` returns the differential flux of neutrinos in `[1/Year/km2/GeV]`, and

`displaySpectrum(nu,"nu from Sun [1/Year/km2/GeV]",Emin,Emax,1)`

allows to display the corresponding spectrum on the screen.

- `muonUpward(nu,Nu,rho, muon)`

calculates the muon flux which results from interactions of neutrinos with rocks below the detector Eq.(44). Here `nu` and `Nu` are input arrays containing the neutrino/anti-neutrino fluxes calculated by `neutrinoFlux`. `rho` is the Earth density  $\approx 2.6g/cm^3$ . `muon` is an array which stores the resulting sum of  $\mu^+$ ,  $\mu^-$  fluxes. `SpectdNdE(E,muon)` gives the differential muon flux in `[1/Year/km2/GeV]` units.

- `muonContained(nu,Nu,rho, muon)` calculates the flux of muons produced in a given detector volume, Eq.(40). This function has the same parameters as `muonUpward` except

that the outgoing array gives the differential muon flux resulting from neutrinos converted to muons in a  $km^3$  volume given in  $[1/\text{Year}/km^3/\text{GeV}]$  units. `rho` is the density of the detector in  $g/cm^3$ .

Two functions allow to estimate the background from atmospheric neutrinos creating muons after interaction with rocks below the detector or with water inside the detector.

- `ATMmuonUpward(cosFi, E)` calculates the sum of muon and anti-muon fluxes that result from interaction of atmospheric neutrinos with rocks. Units are  $[1/\text{Year}/km^2/\text{GeV}/\text{Sr}]$ . `cosFi` is the angle between the direction of observation and the center of the Earth. `E` is the muon energy in GeV.

- `ATMmuonContained(cosFi, E, rho)` calculates the flux of muons caused by atmospheric neutrinos which are produced in a given detector volume in  $[1/\text{Year}/km^3/\text{GeV}]$ . `rho` is the density of the detector in  $[g/cm^3]$ . `cosFi` and `E` are the same as above.

## 4 Dark matter detection

The modules to compute the direct and indirect detection rates are described in Refs. [67, 68]. Here we just mention the few upgrades including improved values for the quark coefficient in nucleons relevant for direct detection, a new module to compute loop-induced annihilation of neutralinos into gauge bosons in the NMSSM and CPVMSSM and new functions for introducing DM clumps.

### 4.1 Gamma-Ray line

The annihilation of a pair of dark matter particles into photon pairs, or  $\gamma Z$  gives a very distinctive DM signal, a monochromatic line at an energy  $E = m_{DM}$  for  $\gamma\gamma$  or  $E = m_{DM}(1 - m_Z^2/4m_{DM}^2)$  for  $\gamma Z$ . Possible evidence for such lines in FermiLAT data have been reported [10, 11] although the result is not yet confirmed by the FermiLAT collaboration and the DM origin of these lines remains to be established. Such processes occur at the one-loop level and are therefore not computed in CalcHEP for generic models. However a module for computing loop-induced neutralino pair annihilation processes in the MSSM ( $\chi\chi \rightarrow \gamma\gamma, \gamma Z$ ) was provided in previous `micrOMEGAs` versions [69]. The code to compute the amplitudes was obtained with `SloopS`, an automatic code for one-loop calculations in the context of the SM and the MSSM [70, 71]. In this version, a similar module is provided for the NMSSM [72] and the CPVMSSM using `SloopS`. The resulting routine, `1Gamma.exe`, reads the [N/CPV]MSSM parameters from an SLHA file, and computes the cross sections for  $\chi\chi \rightarrow \gamma\gamma, \gamma Z$ .

The calculation of  $\chi\chi \rightarrow \gamma\gamma, \gamma Z$  is based on the same functions for all MSSM-like models,

- `int loopGamma(double *vcs_gz, double *vcs_gg)`

If the call was successful this function returns zero and assigns to the variables `vcs_gz` and `vcs_gg` the cross sections  $\sigma v$  for  $\gamma Z$  and  $\gamma, \gamma$  in  $[cm^3/s]$ . The function `gammaFlux` can then be used to calculate the photon fluxes, see example in `main.c` [F]. Note that to activate the calculation of `loopGamma` one has to uncomment the statement

```
#define LoopGAMMA
```

at the top of the file `main.c` [F].

## 4.2 Dark matter profile and clumps

The indirect DM detection signals depend on the DM density in our Galaxy. The DM density is given as the product of the local density at the Sun with the halo profile function

$$\rho(r) = \rho_{\odot} F_{halo}(r) \quad (46)$$

In `micrOMEGAs`  $\rho_{\odot}$  is a global parameter `rhoDM` and the Zhao profile [73]

$$F_{halo}(r) = \left(\frac{R_{\odot}}{r}\right)^{\gamma} \left(\frac{r_c^{\alpha} + R_{\odot}^{\alpha}}{r_c^{\alpha} + r^{\alpha}}\right)^{\frac{\beta-\gamma}{\alpha}} \quad (47)$$

with  $\alpha = 1, \beta = 3, \gamma = 1, r_c = 20[kpc]$  is used by default.  $R_{\odot}$ , the distance from the Sun to the galactic center, is also a global parameter, `Rsun`. The parameters of the Zhao profile can be reset by

- `setProfileZhao( $\alpha, \beta, \gamma, r_c$ )`

The functions to set another density profile reads

- `setHaloProfile( $F_{halo}(r)$ )`

where  $F_{halo}(r)$  is any function from distance from Galactic center,  $r$  has to be defined in [kpc] units. For instance, `setHaloProfile(hProfileEinasto)` sets Einasto profile

$$F_{halo}(r) = \exp\left[-\frac{2}{\alpha} \left(\left(\frac{r}{R_{\odot}}\right)^{\alpha} - 1\right)\right]$$

where by default  $\alpha = 0.17$ , but can be changed by

- `setProfileEinasto( $\alpha$ )`

The command `setHaloProfile(hProfileZhao)` sets back Zhao profile. Note that both `setProfileZhao` and `setProfileEinasto` call `setHaloProfile` to install the corresponding profile.

Dark matter annihilation in the Galaxy depends on the average of the square of the DM density,  $\langle \rho^2 \rangle$ . This quantity can be significantly larger than  $\langle \rho \rangle^2$  when clumps of DM are present [74]. In `micrOMEGAs`, we use a simple model where  $f_{cl}$  is a constant that characterizes the fraction of the total density due to clumps and where all clumps occupy the same volume  $V_{cl}$  and have a constant density  $\rho_{cl}$ . Then assuming clumps do not overlap, we get

$$\langle \rho^2 \rangle = \rho^2 + f_{cl} \rho_{cl} \rho. \quad (48)$$

This simple description allows to demonstrate the main effect of clumps: far from the Galactic center the rate of DM annihilation falls as  $\rho(r)$  rather than as  $\rho(r)^2$ . The parameters  $\rho_{cl}$  and  $f_{cl}$  have zero default values. The routine to change these values is

- `setClumpConst( $f_{cl}, \rho_{cl}$ )`

To be more general, one could assume that  $\rho_{cl}$  and  $f_{cl}$  depend on the distance from galactic center. The effect of clumping is then described by the equation

$$\langle \rho^2 \rangle (r) = \rho(r)(\rho(r) + \rho_{clump}^{eff}(r)) \quad (49)$$

and the function

- `setRhoClumps( $\rho_{clump}^{eff}$ )`

allows to implement a more sophisticated clump structure.

### 4.3 Direct detection

The computation of the direct detection rate was presented in [67]. One important theoretical uncertainty in the direct detection rate comes from the quark coefficients in the nucleon, and in particular the strange quark content. For SI interactions the operator  $\langle N|m_q\bar{\psi}_q\psi_q|N\rangle$  is interpreted as the contribution of the quark  $q$  to the nucleon mass,  $M_N$  with

$$\langle N|m_q\bar{\psi}_q\psi_q|N\rangle = f_q^N M_N \quad (50)$$

We define the operators

$$\sigma_{\pi N} = m_l \langle p|\bar{u}u + \bar{d}d|p\rangle \quad (51)$$

$$\sigma_s = m_s \langle p|\bar{s}s|p\rangle \quad (52)$$

where  $m_l = (m_u + m_d)/2$ . The relative importance of strange quark in nucleon is described by the ratio

$$y = \frac{2\langle p|\bar{s}s|p\rangle}{\langle p|\bar{u}u + \bar{d}d|p\rangle} = \frac{m_l}{m_s} \frac{2\sigma_s}{\sigma_{\pi N}} \quad (53)$$

In earlier `micrOMEGAs` versions, the strange quark content was extracted using the operator  $\sigma_0 = m_l \langle p|\bar{u}u + \bar{d}d - 2\bar{s}s|p\rangle$ , this method leads to large uncertainties in the strange quark content and in the direct detection rate [75, 76]. Recent lattice QCD calculations have allowed a direct determination of  $\sigma_s$  (see [77]), thus reducing significantly the large uncertainty in the estimation of  $y$ , furthermore the central value for  $\sigma_s$  is also rather small. A compilation of recent lattice results is presented in Table 1. Taking the weighted mean of these values ( $\sum x_i/\sigma_i^2 / \sum 1/\sigma_i^2$ ) we get

$$\sigma_s = 42 \pm 5 \text{ MeV} \quad \text{and} \quad \sigma_{\pi N} = 34 \pm 2 \text{ MeV}. \quad (54)$$

Considering the better and more direct determination of  $\sigma_s$  it is more convenient to set the quark from factor from  $\sigma_s$  rather than from  $\sigma_0$ , other parameters are  $m_u/m_d, m_s/m_d, \sigma_{\pi N}$ . The quark coefficients are expressed as

$$f_d^p = \frac{2\sigma_{\pi N}}{\left(1 + \frac{m_u}{m_d}\right) m_p (1 + \alpha)} \quad f_u^p = \frac{m_u}{m_d} \alpha f_d^p \quad f_s^p = \frac{\sigma_s}{m_p} \quad (55)$$

where

$$\alpha = \frac{\langle N|\bar{u}u|N\rangle}{\langle N|\bar{d}d|N\rangle} = \frac{2z - (z-1)y}{2 + (z-1)y} \quad \text{and} \quad z = \frac{\langle N|\bar{u}u|N\rangle - \langle N|\bar{s}s|N\rangle}{\langle N|\bar{d}d|N\rangle - \langle N|\bar{s}s|N\rangle} \approx 1.49 \quad (56)$$

A new function to compute the quark coefficients is defined,

- `calcScalarQuarkFF( $m_u/m_d, m_s/m_d, \sigma_{\pi N}, \sigma_s$ )`

computes the scalar coefficients for the quark content in the nucleon from the quark mass ratios  $m_u/m_d, m_s/m_d$  as well as from  $\sigma_{\pi N}$  and  $\sigma_s$ . The default values given in Table 3 in the Appendix are obtained from the central values  $\sigma_s = 42\text{MeV}, \sigma_{\pi N} = 34\text{MeV}$  in Eq. 54 and from  $m_u/m_d = 0.56, m_s/m_d = 20.2$  [78]. Note that the mass ratios estimated from lattice results rather than from chiral perturbation theory are somewhat different  $m_u/m_d = 0.46 \pm 0.05, m_s/m_d = 27.5 \pm 0.3$  [78].

Table 1: Nucleon coefficients

$\sigma_s$ (MeV)	$\sigma_{\pi N}$ (MeV)	Reference
$8 \pm 21$		[79]
$43 \pm 10$		[80]
$54 \pm 8$		[81]
$22 \pm 37$		[79]
$31 \pm 16$	$50 \pm 10$	[82]
$34^{+31}_{-27}$	$42^{+21}_{-6}$	[83]
$70 \pm 68$	$31 \pm 5$	[84]
$22 \pm 20$	$32 \pm 2$	[85]
$21^{+44}_{-6}$	$45 \pm 6$	[86]
$125 \pm 59$	$43 \pm 6$	[87]
$50 \pm 18$		[88]
	$37 \pm 10$	[89]

## 5 The Higgs sector at colliders

The LEP, Tevatron and LHC colliders have performed extensive searches for the Higgs boson(s). Recently the LHC has announced the discovery of a Higgs-like particle with a mass  $m_h = 125.5\text{GeV}$ . [19, 20] A signal was found notably in the two-photon channel and in the two gauge bosons decay modes. The observation of this new particle as well as the non-observation of a Higgs particle in many other channels at the LHC, LEP or Tevatron both put strong constraints on the parameter space of the extensions of the standard model. Two new features of `micrOMEGAs` allow to compute more precisely the partial widths of the Higgs: the partial width for the Higgs into off-shell W/Z's are included following the approach discussed in section 2.4 and loop-induced couplings of the Higgs are included via effective vertices.

### 5.1 Loop-induced Higgs production and decay

The loop-induced couplings of the Higgs to gluons and photons play an important role in Higgs production and decay at colliders. Thus the `micrOMEGAs` models which are based on tree-level vertices need to be extended to include these interactions. For this we introduce effective operators of the form  $\lambda h F_{\mu\nu} F^{\mu\nu}$  for the CP even part and  $\lambda' h F_{\mu\nu} \tilde{F}^{\mu\nu}$  for the CP-odd part<sup>7</sup>. These operators receive contributions from charged scalars, vector bosons or fermions. For a generic Lagrangian describing the Higgs interactions with fermions  $\psi$ , scalars  $\phi$  and vector bosons  $V^\mu$ ,

$$\mathcal{L} = g_{h\psi\psi} \bar{\psi}\psi h + i g'_{h\psi\psi} \bar{\psi}\gamma_5\psi h + g_{h\phi\phi} M_\phi h \phi\phi + g_{hVV} M_V h V_\mu V^\mu \quad (57)$$

<sup>7</sup>These operators are also used in CalcHEP [90]

the contribution to the effective operators read

$$\begin{aligned} \lambda = & \frac{\alpha}{8\pi} \left[ g_{h\psi\psi} f_\psi^c q_\psi^2 \frac{1}{M_\psi} A_{1/2}\left(\frac{M_h^2}{4M_\psi^2}\right) - g_{hVV} f_V^c q_V^2 \frac{1}{2M_V} A_1\left(\frac{M_h^2}{4M_V^2}\right) \right. \\ & \left. + g_{h\phi\phi} f_\phi^c q_\phi^2 \frac{1}{2M_\phi} A_0\left(\frac{M_h^2}{4M_\phi^2}\right) \right] \end{aligned} \quad (58)$$

and

$$\lambda' = \frac{\alpha}{16\pi} g'_{h\psi\psi} f_\psi^c q_\psi^2 \frac{1}{M_\psi} \tilde{A}_{1/2}\left(\frac{M_h^2}{4M_\psi^2}\right) \quad (59)$$

where  $q$  is the electric charge of the virtual particle for  $\gamma\gamma$  operators and is 1 for the gluon operator,  $f^c$  is the color factor associated with the virtual particle. For the fundamental SU(3) representation  $f^c = 3$  for  $\gamma\gamma$  and  $f^c = 1/2$  for  $gg$ . For the adjoint representation  $f^c = 8$  for photons and  $f^c = -2$  for gluons. The functions  $A_{1/2}, A_1, A_0, \tilde{A}_{1/2}$  are defined in [91, 92].

There are important QCD corrections to the effective vertices with coloured particles in the loop. For  $h\gamma\gamma$  the QCD corrections are described as an overall factor

$$1 + \frac{\alpha_s(M_h/2)}{\pi} C_l \left( \frac{M_h^2}{4M_l^2} \right) \quad (60)$$

where  $M_l$  is the mass of the particle in the loop and the  $C_l$  functions are known for fermions and scalars in the fundamental representation of SU(3). The code HDECAY [93] is used to generate tables for these functions.

The QCD corrections to  $hgg$  to order  $\alpha_s^3$  have been computed in the limit of a heavy top quark. These include both vertex corrections and corrections from gluon emission [94]. The corrections are therefore split into a radiation factor and a vertex factor. For lighter quarks or for new colored particles, only NLO vertex corrections are known. To take into account QCD corrections for all colored fermions and scalars in the loop, we use the following prescription. We use a common radiation factor,  $R$ , for all colored particles and introduce additional correction factors in the amplitude for top/heavy new quarks ( $C_t$ ), light quarks ( $C_q$ ) or colored scalars ( $C_s$ ). The  $hgg$  vertex including QCD corrections for SM fermions and colored scalars (such as squarks in the MSSM) thus reads

$$\lambda_{\text{QCD}} = -R \left[ A_{htt}^{LO} C_t + (A_{hbb}^{LO} + A_{hcc}^{LO}) C_q + \sum_{\tilde{q}} A_{h\tilde{q}\tilde{q}}^{LO} C_{\tilde{q}} \right], \quad (61)$$

where  $A_{hXX}^{LO}$  denote the contribution of particle  $X$  to Eq. 58. The QCD factors with  $a = \alpha_s(Q)/\pi$ , read [94],

$$R^2 = 1 + \frac{149}{12} a + 68.648 a^2 - 212.447 a^3, \quad (62)$$

and

$$C_t = 1 + \frac{11}{4}a + (6.1537 - 2.8542 \log\left(\frac{m_t^2}{Q^2}\right))a^2 + (10.999 - 17.93 \log\left(\frac{m_t^2}{Q^2}\right) + 5.47 \log\left(\frac{m_t^2}{Q^2}\right)^2)a^3 \quad (63)$$

$$C_q = 1 + \frac{11}{4}a \quad (64)$$

$$C_{\bar{q}} = 1 + \frac{9}{2}a, \quad (65)$$

where  $Q = M_h/2$ . The top contribution to the  $hgg$  partial widths agrees with Ref. [94] to order  $\alpha_s^3$ . Our approach which consists in a modification of the effective  $h\gamma\gamma$  and  $hgg$  vertices, necessarily incorporates only part of the higher order corrections to the partial widths (for example for lighter quarks the contribution to order  $\alpha_s$  are taken into account while only some of the  $\alpha_s^2$  contributions are included). Furthermore with the effective vertex approach we cannot introduce QCD corrections for the interference term between two contributions. It is therefore expected that we will have differences with other treatment of QCD corrections. We indeed observe some differences with HDECAY. For instance for lighter quarks or for new particles, the QCD factor in the partial width is in agreement with HDECAY only to order  $\alpha_s$ . Nevertheless for a SM Higgs of 126 GeV, differences with HDECAY are below the percent level. For the SM-like Higgs of the MSSM, differences are also generally small (at the few percent level). Larger discrepancies can be found for the heavier Higgs of the MSSM, in particular when the parameters are chosen such that there is a strong interference between the top and stop contribution. In supersymmetric models, higher-order SUSY corrections, the so-called  $\Delta m_b$  corrections, are taken into account by a redefinition of the  $h\bar{b}b$  vertex. These are also included in `micrOMEGAs` when defining the b-quark contribution to  $h\gamma\gamma$  and  $hgg$ , such corrections are not included in the loop-induced processes in HDECAY thus leading to discrepancies between the two codes when the b-quark contribution is important.

In most extensions of the standard model, the Higgs sector contains several doublets and/or singlets. For all Higgs scalars and pseudoscalars, we follow the same procedure for computing the  $H\gamma\gamma$  and  $Hgg$  vertices, including QCD corrections. Note however that these corrections were obtained in the heavy top quark limit which would not be appropriate for the Higgses that are very heavy. Nevertheless we use these results for all masses, since a high precision is not essential for the loop-induced processes when the Higgs is very heavy, indeed both the gluon fusion Higgs production and the decay in the  $\gamma\gamma$  mode are suppressed at large masses.

The functions that can be used to compute the effective Higgs vertices are

- `HggF(Q)`, `HggS(Q)`, `HggV(Q)`

to compute the fermion/scalar/vector loop contribution to the  $hgg, h\gamma\gamma$  vertices,  $Q = (M_h/2M)^2$  where  $M$  is the mass of the fermion/scalar/vector in the loop.

- `HggA(Q)`

to compute the fermion loop contribution to the  $Agg, A\gamma\gamma$  vertices,  $Q$  is defined as above.

- `Hgam1F(Q)`, `Hgam1S(Q)`

QCD corrections to the fermion/scalar contribution to the  $h\gamma\gamma$  effective vertex, see Eq. 60.

- Hgam1A(Q)

QCD corrections to the fermion contribution to the  $A\gamma\gamma$  effective vertex, see Eq. 60.

Implementation of the loop-induced vertices can be realised using LanHEP, the necessary functions are described next.

## 5.2 Implementation of effective vertices

A new feature in LanHEP allows to extract the expression from any generated vertex. This can be used to implement the different contributions to the loop-induced  $H\gamma\gamma$  and  $Hgg$  vertices. The function which allows to extract a specific coupling is

`CoefVrt([ particles ], [ options ])`,

where *particles* is the comma-separated list of particles in the vertex, and *options* specifies the tensor structure of the required coefficient as well as other options. The only tensor structure that can be extracted are  $1, \gamma^5, \gamma^\mu, \gamma^\mu\gamma^5, p^\mu$  and the function `CoefVrt` must be called separately for each tensor structure. The second list can contain the following symbols in any order:

- `gamma` corresponds to only  $\gamma^\mu$  matrices in the vertex, `gamma5` to only  $\gamma^5$  matrices and `gamma, gamma5` to product of  $\gamma^\mu\gamma^5$  matrices. If none of these symbols are listed, then only terms which do not include  $\gamma$ -matrices will be extracted;
- `moment( P )` where *P* is a particle name selects the terms depending on this particle momentum, note that vertices corresponding to higher order operators and containing the product of several momenta cannot be handled;
- `re, im` - take real or imaginary part of the expression. It can be combined with options above.
- `abbr` - use abbreviations in the returned expressions, this option is useful for long expressions.

The following example illustrates how LanHEP can be used to compute the sleptons contribution to the  $h \rightarrow \gamma\gamma$  effective vertex in supersymmetry. First, we define terms depending on the loop functions :

```
_p=[eL,eR,mL,mR,l1,l2] in parameter rhS__p=creal(HggS((Q/2/MS_p)**2)),
ihS__p=cimag(HggS((Q/2/MS_p)**2)).
```

Here `eL,...l2` are the names for the three generations of charged sleptons, `MSeL...MSl2` are their masses, and we declare the new parameters `rhS_eL...ihS_l2`. The function `HggS` describes the loop integrals in Eq. 58. Then we obtain expressions from the vertices of the Higgs boson interaction with these sleptons (divided by the square of the slepton mass):

```
_p=[eL,eR,mL,mR,l1,l2] in parameter AhS__p=CoefVrt([anti(_p),_p,h])
/(mass _p)**2/2.
```

Note that in general it is preferable to specify whether one wants to extract the real or imaginary part of the vertex, this option was omitted here because we know that this vertex is real. Similarly the option `abbr` is useful to get a compact expression for the vertices involving staus. The charge of particles can, for example, be defined as

`_p in [eL,eR,mL,mR,l1,l2] alias Q(_p)=-1`

Finally, the contribution to the Higgs decay amplitude reads:

```

LAAhs=cabs((rhS_#s1+i*ihS_#s1)*AhS_#s1*Q(s1)*Q(s1)
            where s1=[eL,eR,mL,mR,l1,l2]).

```

In this statement the inner `where` keyword is used to make the sum of expressions where the list of symbols on the right-hand side is substituted into the template expression on the left-hand side. The `#` sign means concatenation of the symbols to the left-hand and right-hand side. To this expression, one must in general add the relevant color factor that appear in Eq. 58 as well as the QCD factors in Eq. 61.

### 5.3 Higgs couplings and Higgs exclusion

In addition to a measurement of the Higgs mass, the LHC collaborations provide estimates of the signal strength ( $\mu$ ) as compared to the SM expectation in various channels. For example for the two-photon decay of a Higgs produced via gluon fusion(ggF) or vector boson fusion(VBF)

$$\mu_{\gamma\gamma}^{ggF} = \frac{\sigma(gg \rightarrow h)_{NP} Br(h \rightarrow \gamma\gamma)_{NP}}{\sigma(gg \rightarrow h)_{SM} Br(h \rightarrow \gamma\gamma)_{SM}} \quad u_{\gamma\gamma}^{VBF} = \frac{\sigma(WW \rightarrow h)_{NP} Br(h \rightarrow \gamma\gamma)_{NP}}{\sigma(WW \rightarrow h)_{SM} Br(h \rightarrow \gamma\gamma)_{SM}} \quad (66)$$

where NP stands for the new physics model under consideration. The ratio of the Higgs partial widths can be obtained easily from the coupling squared normalized to the SM coupling

$$c_{hXX} = g_{hXX}^2(NP)/g_{hXX}^2(SM) \quad (67)$$

and similarly for loop-induced processes,

$$c_{hGG} = \lambda_{hGG}^2(NP)/\lambda_{hGG}^2(SM) \quad (68)$$

where  $G = g, \gamma$  and  $\lambda_{hGG}$  are given in Eqs. 58,60,61. We make the approximation that the ratio of the production cross section is given by the ratio of partial widths even though the QCD correction factors can differ in both cases. For example, the signal strength is thus given by

$$\mu_{\gamma\gamma}^{ggF} = c_{hgg} c_{h\gamma\gamma} \frac{\Gamma_{SM}}{\Gamma_{NP}} \quad (69)$$

The reduced couplings as well as all Higgs partial widths are computed within `micrOMEGAS` and are provided in a SLHA file, `HB.slha`. The total width for the SM, necessary to compute Higgs branching ratios, can be computed from reduced couplings and the total width in the NP model.

To obtain the limits on the Higgs sector for models with more than one Higgs boson, the results for Higgs signal strengths in different channels described above can be compared to the latest results of the LHC. Alternatively an interface to the public code `HiggsBounds` [?] which allows to take into account the exclusion limits provided by the experimental collaborations for many different channels is provided. In `micrOMEGAS`, the interface to `HiggsBounds` is realized via SLHA files, using the effective coupling option for specifying the input. More specifically the file `HB.slha` contains the normalized couplings squared of the Higgs to all SM particles, including the normalized couplings squared to

$\gamma\gamma, \gamma Z, gg$  <sup>8</sup> as well all Higgs partial widths and the top decay width. A reference value is defined for the couplings that do not exist in the standard model, for example the reference value for the Z couplings to two Higgses,  $g_{H^2HZ}^2 = (e/2s_w c_w)^2$ . In the MSSM, analytical formulas for the effective couplings normalized to the SM ones are used for  $h, H, A \rightarrow f\bar{f}, WW, ZZ$  while loop-induced couplings,  $h, H, A \rightarrow \gamma\gamma, gg$ , are computed using the formulas given above. The same procedure is used for most of the models we provide. In the CPVMSSM, the only difference is that loop-induced couplings are computed with CPsuperH. In the NMSSM, we have two options for the Higgs sector : collider constraints can be computed with NMSSMTools or with HiggsBounds. As for other models, the normalized Higgs couplings squared are provided in the `Hb.slha` file.

The SLHA file is then fed to HiggsBounds and the output of HiggsBounds is read using the `slhaVal` function [34]. Note that the output of HiggsBounds consist of two numbers, `HBresult` and `obsratio` which indicate whether a point has been excluded at the 95%*C.L.* by one of the experimental results considered.

HBresult	obsratio	
0	> 1	parameter point is excluded
1	< 1	parameter point is not excluded
-1	< 0	invalid parameter point

Information on the most constraining channel is also given as output. In Section 7 we describe simple tools for reading the SLHA output of HiggsBounds.

In a generic model implemented by the user, the effective Lagrangian for  $h\gamma\gamma$  and  $hgg$  have to be included in the model file as described in section 5.1. Furthermore if one wants to use the HiggsBounds interface, an SLHA file containing the normalized couplings squared must also be provided by the user. In models available in `micrOMEGAs`, the following function can be used for this purpose

- `HBblocks("filename")`

writes at the end of an SLHA file, the new Blocks that contain the effective couplings of the Higgses normalized to the SM ones.

## 6 Dark matter models

Several models are included in the `micrOMEGAs` distribution: the MSSM and some of its extensions (NMSSM and CPVMSSM), the little Higgs model (LHM) [?], a model with a right-handed neutrino (RHN) [35], the inert doublet model (IDM), a model with an extended scalar sector and a  $Z_3$  symmetry (Z3ID) [29, 37] as well as a model with a fourth generation of leptons (SM4). All but the last three models were available in previous versions. All models have been extended to include effective  $h_i gg$  and  $h_i \gamma\gamma$  vertices for all Higgses in the model and to output a file containing reduced Higgs couplings (`Hb.slha`) - the only exception is the RHN which features SM Higgs couplings. Both the MSSM and NMSSM have been updated, we briefly describe the main new features of these models. A more complete description of all models will appear as a separate publication [96]. A model independent calculation of the DM signals is also available.

---

<sup>8</sup>The coupling  $H_i \rightarrow \gamma Z$  will be included in a future release

## 6.1 MSSM

The model files were regenerated using SLHAplus [97] and feature an improved Higgs sector which includes

- Effective vertices for  $Hgg$  and  $H\gamma\gamma$  where  $H = h, H, A$ .
- Threshold corrections for  $\tau$ 's in addition to those for b-quarks [98, 99].
- Improved Higgs effective potential: as in previous versions we write an effective Lagrangian to introduce in a gauge invariant manner the higher-order corrections to the Higgs masses and couplings. The effective scalar potential contains seven parameters ( $\lambda_i$ ) [100], analytic formulas are used to compute  $\lambda_1, \lambda_3, \lambda_6$  [101, 93] other  $\lambda$ 's are computed from these and the four Higgs masses,  $m_h, m_H, m_A, m_{H^\pm}$  given by the spectrum calculator. This improvement has an impact on the Higgs self-couplings, the effect on the DM relic density is however negligible.
- The mass limit function checks that the Higgs mass is in the range  $123 < m_h < 128$  GeV consistent with the LHC results and allowing for a theoretical uncertainty. A warning is issued if this is not the case. The Higgs couplings are not explicitly checked.

Other new features of the MSSM model

- The default spectrum generator has been updated to Suspect\_2.4.1
- In addition to the CMSSM (called SUGRA), AMSB, and EWSB, the user can choose to work with non-universal Higgs masses at the GUT scale (SUGRANUH). The scalar Higgs masses are not used as input parameters, rather they are replaced by  $\mu$ , defined at the EW symmetry breaking scale and the pseudoscalar pole mass,  $m_A$ . The input parameters are therefore  $m_0, m_{1/2}, A_0, \tan\beta, \mu, m_A$  in addition to the optional standard model parameters  $m_t, m_b(m_b), \alpha_s(m_Z)$ . Defining input parameters at different scales follows the standard in SLHA2 [102].
- We have updated the routine for  $b \rightarrow s\gamma$  in order to reproduce the SM value at NNLO, default values for all parameters are given in the online manual.
- We have added three flavor observables in the Kaon and D-meson systems, the leptonic decays,  $K^+ \rightarrow \mu\nu$  and  $D_s \rightarrow \mu\nu, \tau\nu$  as described below. Note that these constraints are also available via the SuperIso interface [103].

The two-body kaon leptonic decays receive a contribution from the charged Higgs at tree-level. However uncertainties in the Kaon parameters are very large, we therefore compute only a quantity that has much smaller uncertainties. This is defined as [104]

$$R_{l23} = \left[ 1 - \frac{m_K^2}{m_{H^\pm}^2} \left( 1 - \frac{m_d}{m_s} \right) \frac{\tan\beta^2}{1 + \epsilon_0 \tan\beta} \right] \quad (70)$$

with  $m_K = 0.494$  GeV and  $m_d/m_s = 1/20.2$ . Here the dependence on the supersymmetric parameters arises at higher order in perturbation theory (through the  $\epsilon_0$  term) but can be large because of the  $\tan\beta$  enhancement,

$$\epsilon_0 = -\frac{2\alpha_s\mu}{3\pi m_{\tilde{g}}} H_2\left(\frac{m_{\tilde{q}_L}^2}{m_{\tilde{g}}^2}, \frac{m_{\tilde{d}_R}^2}{m_{\tilde{g}}^2}\right) \quad (71)$$

The measured value for this quantity is  $R_{l23} = 1.004 \pm 0.007$  [104].

The branching ratios  $D_s \rightarrow \tau\nu$  and  $D_s \rightarrow \mu\nu$  also receive a contribution from the charged Higgs, [105]

$$Br(D_s \rightarrow l\nu) = \frac{G_F^2}{8\pi} |V_{cs}|^2 f_{D_s}^2 m_l^2 m_{D_s} \tau_{D_s} \left(1 - \frac{m_l^2}{m_{D_s}^2}\right)^2 \times \left[1 + \frac{1}{1 + \frac{m_s}{m_c}} \frac{m_{D_s}^2}{m_{H^\pm}^2} \left(1 - \frac{m_s}{m_c} \frac{\tan^2 \beta}{1 + \epsilon_0 \tan \beta}\right)\right]^2 \quad (72)$$

with  $\epsilon_0$  as in Eq. 71 with  $m_{\tilde{d}_R} \rightarrow m_{\tilde{c}_R}$ . These branching ratios were measured recently, [106]

$$\begin{aligned} Br(D_s \rightarrow \tau\nu) &= (5.44 \pm 0.22) \times 10^{-2} \\ Br(D_s \rightarrow \mu\nu) &= (5.54 \pm 0.24) \times 10^{-3} \end{aligned} \quad (73)$$

## 6.2 NMSSM

The NMSSM model files have also been updated and a new interface to NMSSMTools\_4.0 [30] is provided. Thus all new features of NMSSMTools [30, 31] are included, in particular the computation of reduced Higgs couplings. The main new features of `micrOMEGAs` are:

- Effective vertices for  $Hgg$  and  $H\gamma\gamma$  where  $H = h_i, a_j, i = 1, 3; j = 1, 2$ .
- Improved Higgs effective potential: as in previous versions we write an effective Lagrangian to introduce in a gauge invariant manner the higher-order corrections to the Higgs masses and couplings [107]. The effective scalar potential has been extended to contain more than 20 operators,  $\lambda_i$ 's [?] <sup>9</sup>. Analytic formulas are used to compute the  $\lambda_i$ 's which are then fed to `micrOMEGAs`. The new Higgs self-coupling can in some cases have a large effect on the DM relic density.

## 6.3 Model independent signals

A model independent calculation of the DM observables is also available. After specifying the DM mass, the cross sections for DM spin dependent and spin independent scattering on proton and neutron, the DM annihilation cross section times velocity at rest and the relative contribution of each annihilation channel to the total DM annihilation cross section, one can compute the direct detection rate on various nuclei, the fluxes for photons, neutrinos and antimatter resulting from DM annihilation in the galaxy and the neutrino/muonfluxes in neutrino telescopes.

The functions `nuclearRecoilAux` for the computation of the event rate for direct detection and `basicSpectra` which provides the  $\gamma, p^-, e^+$  and  $\nu$  spectra for different annihilation channels are described in [67], [68]. The fluxes for photons, neutrinos, positrons and antiprotons from DM annihilation in the galaxy are computed using the same functions as in specific models. The new functions that allow for a model independent calculation of the neutrino telescope signal from DM captured are

- `captureAux(f, forSun, csIp, csIn, csDp, csDn)` calculates the number of DM particles captured per second assuming the cross sections

<sup>9</sup>See also Ref. [?] for a general parametrization of the effective scalar potential

for spin-independent and spin-dependent interactions with protons and neutrons `csIp`, `csIn`, `csDp`, `csDn` are given as input parameters (in [pb]). A negative value for one of the cross sections is interpreted as a destructive interference between the proton and neutron amplitudes. The first two parameters have the same meaning as in the `neutrinoFlux` routine Section 3.6. The result depends implicitly on the global parameters `rhoDM` and `Mcdm` in Table 2.

- `basicNuSpectra(forSun, pdgN, outN, nu)`

calculates the  $\nu_\mu$  and  $\bar{\nu}_\mu$  spectra corresponding to DM annihilating into particles specified by the PDG code `pdgN`. Effects of interaction with Sun/Earth medium as well as neutrino oscillation are taken into account [64]. `outN` should be chosen 1 for muon neutrino and -1 for anti-neutrino. The resulting spectrum is stored in the array `nu` with `NZ=250` elements which can be checked by the `SpectdNdE(E, nu)` function.

The annihilation rate for this model independent analysis is obtained from the capture rate using Eq. 36. The function `basicNuSpectra` described above can be used to obtain the neutrino fluxes assuming some user defined value for each channel branching ratio in Eq.(39).

The files `main.c/F` in the directory `mdlIndep` contain an example of the calculation of the direct detection, indirect detection and neutrino telescope signals using the routines described in this section. The numerical input data in this sample file corresponds to 'MSSM/mssmh.dat'.

## 7 External codes in micrOMEGAs

The subdirectory `Packages` in `micrOMEGAs_3.1` contains external public codes such as `SuSpect` [32], `CPsuperH` [33], `HiggsBounds-4.0.0` [?], `LoopTools-2.1` [108]. These external codes are not compiled during the general installation of `micrOMEGAs`, rather they are compiled either when installing a model requiring one of these codes or in runtime of `micrOMEGAs` executables. The `micrOMEGAs` interface to these codes (except for `LoopTools`) is done via files written following the SLHA convention. Routines of the `SLHAplus` package [97] included in `micrOMEGAs` can be used to read the information contained in these files, as in previous versions the following function is available

- `slhaRead(filename, mode)`

reads all or part of the data from the file `filename`. `mode` is an integer which determines which part of the data should be read from the file, `mode= 1*m1+2*m2+4*m4+8*m8+16*m16` where

```

m1 = 0/1 - overwrites all/keeps old data
m2 = 0/1 - ignore errors in input file/ stop in case of error
m4 = 0/1 - read DECAY /do not read DECAY
m8 = 0/1 - read BLOCK/do not read BLOCK
m16 = 0/1 - read QNUMBERS/do not read QNUMBERS

```

For example `mode=20 (m4=1, m16=1)` is an instruction to overwrite all previous data and read only the information stored in the `BLOCK` sections of `filename`. In the same manner `mode=25=1+8+16` is an instruction to add information from `DECAY` to the data obtained previously.

The function `slhaRead` returns the values:

```

0 - successful reading
-1 - can not open file
-2 - invalid data as indicated by SPINFO
-3 - no data
n>0 - wrong file format at line n

```

In SLHA, information is stored in blocks identifiable with the convention: a line starting with the keyword "BLOCK" followed by the name of the block. Each block then contains a list of records, each on a separate line started with space symbol, that give information on physical parameters. The structure of a block record is not defined in SLHA. In the first SLHA implementations, the structure of a block was the following : key parameters defining the variables followed by some numerical parameters giving the value of these variables. For example,

```

BLOCK MASS
6                173.2 # top quark mass
1000022          1.34362460e+02 # ~neutralino(1)

```

New codes have actually introduced new formats for blocks, for example in the *Flavour Les Houches Accord* [109] key parameters are specified both before and after the numerical parameters,

```

Block FOBS # Flavour observables
# ParentPDG type      value      q  NDA ID1  ID2 ID3 ... comment
5           1      2.83249483e-04 0   2   3   22 # BR(b->s gamma)

```

The SLHAplus package [97] was updated to read blocks with any format, in addition to the function `slhaVal`, we have introduced the function

- `slhaValFormat(char * Block, double Q, char * format)`

which allows to extract numerical information corresponding to the key parameter described in *format*. The *format* parameter is actually a C-style format. For instance in the "BLOCK MASS" above, the mass of the neutralino can be obtained by

```
MNE1=slhaValFormat("MASS", 0., " 1000022 %lf");
```

while in the "BLOCK FOBS", the branching  $b \rightarrow s\gamma$  can be obtained by

```
B2sg=slhaValFormat("FOBS", 0., "5 1 %lf  %*f 2 3 22");
```

The parameter  $Q$  is meaningful only for blocks which feature a scale dependence. Note that the number of space symbols in *format* is irrelevant since it has the same properties as the C *scanf* function.

A block can also contain a textual information. For example, in HIGGSBOUNDS a block contains the following records,

```

Block HiggsBoundsResults
#CHANNELTYPE 1: channel with the highest statistical sensitivity
1           1           328           # channel id number
1           2           1           # HBresult
1           3 0.72692779334500290     # obsratio
1           4           1           # ncombined
1           5 ||(p p)->h+..., h=1 where h is SM-like (CMS-PAS-HIG-12-008)|| # text description of channel

```

In particular, the last record contains the name of the channel which gives the strongest constraint on the Higgs. To extract the name of this channel one can use the new function

- `slhaSTRFormat("HiggsBoundsResults","1 5 || %[^|]||",channel);`  
which will write the channel name in text parameter *channel*.

The following packages have been attached to `micrOMEGAs` using the SLHAplus interface: SOFTSUSY [110], SPHENO [111], ISAJET [112], SuperIso [103], SUSY-HIT [113], HDECAY [93], SusyBSG [114].

Note that the `make clean` command launched in the `micrOMEGAs` root directory subsequently calls `make clean` for all sub-directories in the `Packages` directory.

## 8 Installation and running the code

### 8.1 Installation.

To download `micrOMEGAs`, go to

`http://lapth.cnrs.fr/micromegas`

and unpack the file received, `micromegas_3.X.tgz`, with the command

```
tar -xvzf micromegas_3.X.tgz
```

This should create the directory `micromegas_3.X/`. In case of problems and questions please send a mail to `micromegas@lapth.cnrs.fr`.

To compile `CalcHEP` and `micrOMEGAs` go to the `micrOMEGAs` directory and launch `gmake`

The command `make` should work like `gmake` if the latter is not available. In principle `micrOMEGAs` defines automatically the names of *C* and *Fortran* compilers and the flags for compilation. If you meet a problem, open the file which contain the compiler specifications, `CalcHEP_src/FlagsForSh`, improve it, and launch `[g]make` again.

After compilation of `micrOMEGAs` one has to compile the executable to compute DM related observables in a specific model. To do this, go to the model directory, say `MSSM`, and launch

```
[g]make main=main.c
```

It should generate the executable `main`. In the same manner

```
gmake main=filename.ext
```

generates the executable `filename` based on the source file `filename.ext`. For *ext* we support 3 options: *'c'*, *'F'*, *'cpp'* which correspond to C, FORTRAN and C++ sources. `[g]make` called in the model directory automatically launches `[g]make` in subdirectories *lib* and *work* to compile

`lib/aLib.a` - library of auxiliary model functions, e.g. constraints,

`work/work_aux.a` - library of model particles, free and dependent parameters.

Default versions of *main.c/F* programs need some arguments which have to be specified in command lines. If launched without arguments *main* explains which parameter are needed. As a rule *main* needs the name of a file containing the numerical values of the free parameters of the model.

To add a new model to `micrOMEGAs` one has to launch the command

```
./newProject modelName
```

which creates the directory `modelName` which contains all subdirectories and commands required. Then one has to prepare the `CalcHEP` model files and place them in the subdirectory `work/models/`, furthermore auxiliary codes used in the model have to be in-

cluded in the sub-directory `lib/`.

## 8.2 Module structure of main program

Each model included in `micrOMEGAs` is accompanied with sample files for C and Fortran programs which call `micrOMEGAs` routines, the `main.c`, `main.F` files<sup>10</sup>. These files consist of several modules enclosed between the instructions

```
#ifdef KEYWORD
.....
#endif
```

where `KEYWORD` is the name of the module, all modules are completely independent. The user can comment or uncomment any set of *define* instructions to suit his/her need. The following modules are available for all models:

```
MASSES_INFO //Masses and widths of Higgs particles and masses
of particles in the odd sector.
CONSTRAINTS //Checks various constraints.
HIGGSBOUNDS //Calls HiggsBounds to constrain the Higgs sector.
OMEGA //DM Relic density.
INDIRECT_DETECTION //Signals of DM annihilation in the galactic halo.
RESET_FORMFACTORS //Redefinition of nucleon Form Factors.
CDM_NUCLEON //Amplitudes and cross sections for DM-nucleon scattering.
CDM_NUCLEUS //Cross section and recoil energy distribution for
DM-nucleus scattering.
NEUTRINO //Neutrino flux from DM captured in the Sun/Earth
and the corresponding muon flux.
DECAYS //Decay widths and branching ratios.
CROSS_SECTIONS//Cross sections for  $2\to 2$  processes.
CLEAN //Cleans intermediate files.
```

For the three MSSM-like models, a module to calculate neutralino annihilation in  $\gamma\gamma$  and  $\gamma Z$  is also available, it is driven by the `#define LoopGAMMA` instruction.

All models also contain the preprocessor command `#define SHOWPLOTS` which generates various plots in `CalcHEP`. By default it is switched off.

A complete description of all `micrOMEGAs` functions is available in the online manual, see also [34]. This updated manual is also provided with the code, the file `manual13.pdf` can be found in the `micrOMEGAs_3.X/man` directory.

## 8.3 Sample output

Running the `main.c` sample file in the `micrOMEGAs/MSSM` directory choosing the options `MASSES_INFO`, `CONSTRAINTS`, `OMEGA`, `INDIRECT_DETECTION`, `CDM_NUCLEON`, `NEUTRINO`, `DECAYS` and with the `mssmh.par` input file will lead to the following output.

---

<sup>10</sup>The C++ version of the sample main program can be obtained by copying `main.c` to `main.cpp`

===== EWSB scale input =====

Spectrum calculator is suspect

Initial file "mssmh.par"

The following parameters keep default values:

alfSMZ=1.1720E-01	MW=8.0200E+01	MZ=9.1300E+01	Ml=1.7770E+00
McMc=1.2700E+00	MbMb=4.2300E+00	Mtp=1.7350E+02	Au=0.0000E+00
Ad=0.0000E+00	wt=1.4420E+00	wZ=2.5020E+00	wW=2.0940E+00

SU\_read\_leshouches: end of file

OUTPUT in SLHA format in suspect2\_lha.out

RUN TERMINATED : OUTPUT in suspect2.out

Warnings from spectrum calculator:

.....none

Dark matter candidate is '~o1' with spin=1/2 mass=1.89E+02

~o1 = 0.950\*bino -0.062\*wino +0.257\*higgsino1 -0.167\*higgsino2

=== MASSES OF HIGGS AND SUSY PARTICLES: ===

Higgs masses and widths

h	126.08	3.49E-03
H	699.89	5.16E+00
H3	700.00	5.80E+00
H+	704.62	4.74E+00

Masses of odd sector Particles:

~o1	: MNE1 =	189.0		~l1	: MS11 =	198.6		~eR	: MSeR =	204.8
~mR	: MSmR =	204.8		~1+	: MC1 =	283.8		~o2	: MNE2 =	290.0
~o3	: MNE3 =	310.3		~2+	: MC2 =	444.0		~o4	: MNE4 =	444.2
~ne	: MSne =	496.0		~nm	: MSnm =	496.0		~n1	: MSn1 =	496.0
~eL	: MSeL =	502.0		~mL	: MSmL =	502.0		~l2	: MS12 =	502.5
~t1	: MSt1 =	1367.6		~b1	: MSb1 =	1551.8		~b2	: MSb2 =	1565.7
~t2	: MSt2 =	1655.7		~g	: MSG =	1900.2		~uL	: MSuL =	2045.0
~cL	: MScL =	2045.0		~uR	: MSuR =	2045.3		~cR	: MScR =	2045.3
~dR	: MSdR =	2045.8		~sR	: MSsR =	2045.8		~dL	: MSdL =	2046.5
~sL	: MSsL =	2046.5								

==== Physical Constraints: =====

deltarho=3.56E-04

gmuon=1.15E-09

bsgnlo=3.05E-04 ( SM 3.25E-04 )

bsmumu=3.38E-09

btaunu=9.56E-01

dtaunu=5.17E-02 dmunu=5.33E-03

R123=9.998166E-01

MassLimits OK

==== Calculation of relic density =====  
 Xf=2.65e+01 Omega=1.03e-01

Channels which contribute to 1/(omega) more than 1%.  
 Relative contributions in % are displayed

18%  $\tilde{0}1 \tilde{0}1 \rightarrow t T$   
 16%  $\tilde{0}1 \tilde{1}1 \rightarrow A l$   
 10%  $\tilde{0}1 \tilde{0}1 \rightarrow l L$   
 7%  $\tilde{1}1 \tilde{1}1 \rightarrow l l$   
 5%  $\tilde{0}1 \tilde{1}1 \rightarrow Z l$   
 5%  $\tilde{0}1 \tilde{e}R \rightarrow A e$   
 5%  $\tilde{0}1 \tilde{m}R \rightarrow A m$   
 4%  $\tilde{0}1 \tilde{0}1 \rightarrow b B$   
 4%  $\tilde{0}1 \tilde{0}1 \rightarrow e E$   
 4%  $\tilde{0}1 \tilde{0}1 \rightarrow m M$   
 3%  $\tilde{e}R \tilde{1}1 \rightarrow e l$   
 3%  $\tilde{m}R \tilde{1}1 \rightarrow m l$   
 2%  $\tilde{0}1 \tilde{0}1 \rightarrow W^+ W^-$   
 2%  $\tilde{1}1 \tilde{L}1 \rightarrow A A$   
 1%  $\tilde{0}1 \tilde{e}R \rightarrow Z e$   
 1%  $\tilde{0}1 \tilde{m}R \rightarrow Z m$   
 1%  $\tilde{1}1 \tilde{L}1 \rightarrow A Z$   
 1%  $\tilde{0}1 \tilde{0}1 \rightarrow Z Z$

==== Indirect detection =====

Channel	vcs[cm <sup>3</sup> /s]
=====	

annihilation cross section	9.22E-27 cm <sup>3</sup> /s
$\tilde{0}1, \tilde{0}1 \rightarrow t T$	5.34E-27
$\tilde{0}1, \tilde{0}1 \rightarrow l L$	1.90E-27
$\tilde{0}1, \tilde{0}1 \rightarrow b B$	1.06E-27
$\tilde{0}1, \tilde{0}1 \rightarrow W^+ W^-$	5.57E-28
$\tilde{0}1, \tilde{0}1 \rightarrow Z Z$	2.56E-28
$\tilde{0}1, \tilde{0}1 \rightarrow Z h$	1.10E-28

sigmav=9.22E-27[cm<sup>3</sup>/s]

Photon flux for angle of sight f=0.00[rad]

and spherical region described by cone with angle 0.0349[rad]

Photon flux = 1.61E-14[cm<sup>2</sup> s GeV]<sup>-1</sup> for E=94.5[GeV]

Positron flux = 5.61E-13[cm<sup>2</sup> sr s GeV]<sup>-1</sup> for E=94.5[GeV]

Antiproton flux = 6.34E-13[cm<sup>2</sup> sr s GeV]<sup>-1</sup> for E=94.5[GeV]

==== Calculation of CDM-nucleons amplitudes =====

CDM-nucleon micrOMEGAs amplitudes:

proton: SI -3.547E-09 SD -2.115E-07

neutron: SI -3.634E-09 SD 1.862E-07

CDM-nucleon cross sections[pb]:

proton SI 5.446E-09 SD 5.807E-05

neutron SI 5.715E-09 SD 4.503E-05

```
=====Neutrino Telescope===== for Sun
E>1.0E+00 GeV neutrino flux      5.783577E+10 [1/Year/km^2]
E>1.0E+00 GeV anti-neutrino flux  6.224851E+10 [1/Year/km^2]
E>1.0E+00 GeV Upward muon flux   2.258430E+02 [1/Year/km^2]
E>1.0E+00 GeV Contained muon flux 1.217184E+03 [1/Year/km^3]
```

```
===== Decays =====
```

h : total width=4.564910E-03

and Branchings:

```
2.549952E-02 h -> Z,Z
2.098720E-01 h -> W+,W-
2.147891E-03 h -> A,A
6.913403E-02 h -> G,G
6.332254E-02 h -> l,L
1.367769E-04 h -> u,U
1.509459E-04 h -> d,D
2.669341E-02 h -> c,C
1.509459E-04 h -> s,S
6.028919E-01 h -> b,B
```

$\tilde{o}2$  : total width=1.357505E-01

and Branchings:

```
4.451636E-02  $\tilde{o}2$  -> Z, $\tilde{o}1$ 
1.225739E-01  $\tilde{o}2$  -> E, $\tilde{e}R$ 
1.225739E-01  $\tilde{o}2$  -> e, $\tilde{e}R$ 
1.225739E-01  $\tilde{o}2$  -> M, $\tilde{m}R$ 
1.225739E-01  $\tilde{o}2$  -> m, $\tilde{m}R$ 
2.325939E-01  $\tilde{o}2$  -> L, $\tilde{l}1$ 
2.325939E-01  $\tilde{o}2$  -> l, $\tilde{l}1$ 
```

## Acknowledgements

We thank C. Hugonie for providing the new NMSSMTools interface. We also thank A. Anandakrishnan, J. Da Silva, G. Drieu La Rochelle, B. Dumont, A. Goudelis, and S. Kulkarni for testing the beta versions of the code. This work was supported in part by the LIA-TCAP of CNRS, by the French ANR, *Programme BLANC/DMAstro-LHC* and was performed within the Labex ENIGMASS. The work of AP was also supported by the Russian foundation for Basic Research, grant RFBR-12-02-93108-CNRSL-a. GB and AP also thank the Galileo Galilei Institute for Theoretical Physics (GGI Florence) for hospitality and the INFN for partial support.

# Appendix

## A Analytical solution of neutrino flux

When DM is not self-conjugate, Eqs. 37 for the number density can be solved analytically if we assume that equilibrium is reached and that the evaporation rate is negligible.

Define

$$\beta = \frac{C_x}{C_{\bar{x}}} ; \alpha = \frac{A_{xx}}{A_{x\bar{x}}} \quad x = \frac{N_x}{N_{\bar{x}}} \quad (74)$$

Then after equilibrium is reached the annihilation rate is determined by the capture rates as well as  $\alpha$ , here we assume  $A_{\bar{x}\bar{x}} = A_{xx}$ ,

$$\begin{aligned} \Gamma_{x\bar{x}} &= \frac{C_x}{1 + \alpha x} \\ \Gamma_{xx} &= \frac{C_x}{2} \left( \frac{x\alpha}{1 + \alpha x} \right) = C_{\bar{x}} \frac{x}{x + \alpha} \\ \Gamma_{\bar{x}\bar{x}} &= \frac{1}{2} C_{\bar{x}} \frac{\alpha}{1 + \alpha x} \end{aligned} \quad (75)$$

where

$$x = \frac{1}{2\alpha} \left[ \beta - 1 \pm ((\beta - 1)^2 + 4\alpha^2\beta)^{1/2} \right] \quad (76)$$

## B Global Parameters

A list of the global parameters and their default values are given in Tables 2, 3. The numerical value for any of these parameters can be simply reset anywhere in the code.

Table 2: Global parameters of `micrOMEGAs`

Name	default value	units	comments
Mcdm		GeV	Mass of Dark Matter particle
deltaY	0		Difference of DM/anti-DM abundances
DMasymm	0		Asymmetry between relic density of DM/anti-DM
K_dif	0.0112	kpc <sup>2</sup> /Myr	The normalized diffusion coefficient
L_dif	4	kpc	Vertical size of Galaxy diffusive halo
Delta_dif	0.7		Slope of diffusion coefficient
Tau_dif	10 <sup>16</sup>	s	Electron energy loss time
Vc_dif	0	km/s	Convective Galactic wind
Fermi_a	0.52	fm	nuclei surface thickness
Fermi_b	-0.6	fm	parameters to set the nuclei radius with
Fermi_c	1.23	fm	$R_A = cA^{1/3} + b$
Rsun	8.5	kpc	Distance from Sun to center of Galaxy
Rdisk	20	kpc	Radius of galactic diffusion disk
rhoDM	0.3	GeV/cm <sup>3</sup>	Dark Matter density at Rsun
Vearth	225.2	km/s	Galaxy velocity of Earth

Table 3: Global parameters of `micrOMEGAs`: nucleon quark form factors

Proton		Neutron		comments
Name	value	Name	value	
ScalarFFPd	0.0191	ScalarFFNd	0.0273	Scalar form factor
ScalarFFPu	0.0153	ScalarFFNu	0.011	
ScalarFFPs	0.0447	ScalarFFNs	0.0447	
pVectorFFPd	-0.427	pVectorFFNd	0.842	Axial-vector form factor
pVectorFFPu	0.842	pVectorFFNu	-0.427	
pVectorFFPs	-0.085	pVectorFFNs	-0.085	
SigmaFFPd	-0.23	SigmaFFNd	0.84	Tensor form factor
SigmaFFPu	0.84	SigmaFFNu	-0.23	
SigmaFFPs	-0.046	SigmaFFNs	-0.046	

## References

- [1] **Planck** Collaboration, P. Ade *et al.*, “Planck 2013 results. XVI. Cosmological parameters,” 1303.5076.
- [2] R. Bernabei *et al.*, “New results from DAMA/LIBRA,” *Eur. Phys. J.* **C67** (2010) 39–49, 1002.1028.
- [3] **CDMS** Collaboration, R. Agnese *et al.*, “Dark Matter Search Results Using the Silicon Detectors of CDMS II,” *Phys.Rev.Lett.* (2013) 1304.4279.
- [4] C. E. Aalseth *et al.*, “Search for an Annual Modulation in a P-type Point Contact Germanium Dark Matter Detector,” *Phys. Rev. Lett.* **107** (2011) 141301, 1106.0650.
- [5] G. Angloher, M. Bauer, I. Bavykina, A. Bento, C. Bucci, *et al.*, “Results from 730 kg days of the CRESST-II Dark Matter Search,” *Eur.Phys.J.* **C72** (2012) 1971, 1109.0702.
- [6] **XENON100** Collaboration, E. Aprile *et al.*, “Dark Matter Results from 225 Live Days of XENON100 Data,” 1207.5988.
- [7] **COUPP** Collaboration, E. Behnke *et al.*, “Improved Spin-Dependent WIMP Limits from a Bubble Chamber,” *Science* **319** (2008) 933–936, 0804.2886.
- [8] S. Archambault *et al.*, “Dark Matter Spin-Dependent Limits for WIMP Interactions on 19-F by PICASSO,” *Phys. Lett.* **B682** (2009) 185–192, 0907.0307.
- [9] **Fermi-LAT** Collaboration, M. Ackermann *et al.*, “Constraining Dark Matter Models from a Combined Analysis of Milky Way Satellites with the Fermi Large Area Telescope,” *Phys.Rev.Lett.* **107** (2011) 241302, 1108.3546.
- [10] T. Bringmann, X. Huang, A. Ibarra, S. Vogl and C. Weniger, *JCAP* **1207** (2012) 054 [arXiv:1203.1312 [hep-ph]].
- [11] C. Weniger, “A Tentative Gamma-Ray Line from Dark Matter Annihilation at the Fermi Large Area Telescope,” *JCAP* **1208** (2012) 007, 1204.2797.
- [12] **Fermi LAT** Collaboration, M. Ackermann *et al.*, “Measurement of separate cosmic-ray electron and positron spectra with the Fermi Large Area Telescope,” *Phys.Rev.Lett.* **108** (2012) 011103, 1109.0521.
- [13] **PAMELA** Collaboration, O. Adriani *et al.*, “An anomalous positron abundance in cosmic rays with energies 1.5-100 GeV,” *Nature* **458** (2009) 607–609, 0810.4995.
- [14] **AMS** Collaboration, M. Aguilar *et al.*, “First Result from the Alpha Magnetic Spectrometer on the International Space Station: Precision Measurement of the Positron Fraction in Primary Cosmic Rays of 0.5-350 GeV,” *Phys.Rev.Lett.* **110** (2013), no. 14, 141102.

- [15] O. Adriani *et al.*, “A new measurement of the antiproton-to-proton flux ratio up to 100 GeV in the cosmic radiation,” *Phys. Rev. Lett.* **102** (2009) 051101, 0810.4994.
- [16] **Super-Kamiokande** Collaboration, T. Tanaka *et al.*, “An Indirect Search for WIMPs in the Sun using 3109.6 days of upward-going muons in Super-Kamiokande,” *Astrophys.J.* **742** (2011) 78, 1108.3384.
- [17] J. Zornoza, “Search for Dark Matter in the Sun with the ANTARES Neutrino Telescope in the CMSSM and mUED frameworks,” 1204.5290.
- [18] **IceCube** Collaboration, R. Abbasi *et al.*, “Multi-year search for dark matter annihilations in the Sun with the AMANDA-II and IceCube detectors,” *Phys.Rev.* **D85** (2012) 042002, 1112.1840.
- [19] **ATLAS** Collaboration, G. Aad *et al.*, “Observation of a new particle in the search for the Standard Model Higgs boson with the ATLAS detector at the LHC,” *Phys.Lett.* **B716** (2012) 1–29, 1207.7214.
- [20] **CMS** Collaboration, S. Chatrchyan *et al.*, “Observation of a new boson at a mass of 125 GeV with the CMS experiment at the LHC,” *Phys.Lett.* **B716** (2012) 30–61, 1207.7235.
- [21] **ATLAS** Collaboration, G. Aad *et al.*, “Search for dark matter candidates and large extra dimensions in events with a photon and missing transverse momentum in  $pp$  collision data at  $\sqrt{s} = 7$  TeV with the ATLAS detector,” *Phys.Rev.Lett.* **110** (2013) 011802, 1209.4625.
- [22] **ATLAS** Collaboration, G. Aad *et al.*, “Search for dark matter candidates and large extra dimensions in events with a jet and missing transverse momentum with the ATLAS detector,” *JHEP* **1304** (2013) 075, 1210.4491.
- [23] **CMS Collaboration** Collaboration, S. Chatrchyan *et al.*, “Search for dark matter and large extra dimensions in monojet events in  $pp$  collisions at  $\sqrt{s} = 7$  TeV,” *JHEP* **1209** (2012) 094, 1206.5663.
- [24] P. Gondolo *et al.*, “DarkSUSY: Computing supersymmetric dark matter properties numerically,” *JCAP* **0407** (2004) 008, astro-ph/0406204.
- [25] H. Baer, A. Belyaev, T. Krupovnickas, and J. O’Farrill, “Indirect, direct and collider detection of neutralino dark matter,” *JCAP* **0408** (2004) 005, hep-ph/0405210.
- [26] A. Arbey and F. Mahmoudi, “SuperIso Relic: A Program for calculating relic density and flavor physics observables in Supersymmetry,” *Comput.Phys.Commun.* **181** (2010) 1277–1292, 0906.0369.
- [27] A. Semenov, “LanHEP - a package for the automatic generation of Feynman rules in field theory. Version 3.0,” *Comput. Phys. Commun.* **180** (2009) 431–454, 0805.0555.

- [28] R. Barbieri, L. J. Hall, and V. S. Rychkov, “Improved naturalness with a heavy Higgs: An Alternative road to LHC physics,” *Phys.Rev.* **D74** (2006) 015007, [hep-ph/0603188](#).
- [29] G. Belanger, K. Kannike, A. Pukhov, and M. Raidal, “Impact of semi-annihilations on dark matter phenomenology - an example of  $Z_N$  symmetric scalar dark matter,” *JCAP* **04** (2012) 010, [1202.2962](#).
- [30] U. Ellwanger and C. Hugonie, “NMHDECAY 2.0: An Updated program for sparticle masses, Higgs masses, couplings and decay widths in the NMSSM,” *Comput.Phys.Commun.* **175** (2006) 290–303, [hep-ph/0508022](#).
- [31] U. Ellwanger and C. Hugonie, “NMSPEC: A Fortran code for the sparticle and Higgs masses in the NMSSM with GUT scale boundary conditions,” *Comput.Phys.Commun.* **177** (2007) 399–407, [hep-ph/0612134](#).
- [32] A. Djouadi, J.-L. Kneur, and G. Moultaka, “SuSpect: A Fortran code for the supersymmetric and Higgs particle spectrum in the MSSM,” *Comput. Phys. Commun.* **176** (2007) 426–455, [hep-ph/0211331](#).
- [33] J. Lee, M. Carena, J. Ellis, A. Pilaftsis, and C. Wagner, “CPsuperH2.3: an Updated Tool for Phenomenology in the MSSM with Explicit CP Violation,” *Comput.Phys.Commun.* **184** (2013) 1220–1233, [1208.2212](#).
- [34] G. Bélanger, F. Boudjema, and A. Pukhov, *micrOMEGAs: A Package for Calculation of Dark Matter Properties in Generic Model of Particle Interaction*, ch. 12, pp. 739–790. World Scientific, 2012. [http://www.worldscientific.com/doi/pdf/10.1142/9789814390163\\_0012](http://www.worldscientific.com/doi/pdf/10.1142/9789814390163_0012).
- [35] G. Belanger, A. Pukhov, and G. Servant, “Dirac Neutrino Dark Matter,” *JCAP* **0801** (2008) 009, [0706.0526](#).
- [36] V. Barger, P. Langacker, M. McCaskey, M. Ramsey-Musolf, and G. Shaughnessy, “Complex Singlet Extension of the Standard Model,” *Phys.Rev.* **D79** (2009) 015018, [0811.0393](#).
- [37] G. Belanger, K. Kannike, A. Pukhov, and M. Raidal, “ $Z_3$  Scalar Singlet Dark Matter,” [1211.1014](#).
- [38] M. L. Graesser, I. M. Shoemaker, and L. Vecchi, “Asymmetric WIMP dark matter,” *JHEP* **1110** (2011) 110, [1103.2771](#).
- [39] H. Iminniyaz, M. Drees, and X. Chen, “Relic Abundance of Asymmetric Dark Matter,” *JCAP* **1107** (2011) 003, [1104.5548](#).
- [40] U. Ellwanger and P. Mitropoulos, “Upper Bounds on Asymmetric Dark Matter Self Annihilation Cross Sections,” *JCAP* **1207** (2012) 024, [1205.0673](#).
- [41] G. Belanger, F. Boudjema, A. Pukhov, and A. Semenov, “micrOMEGAs: Version 1.3,” *Comput. Phys. Commun.* **174** (2006) 577–604, [hep-ph/0405253](#).

- [42] G. Belanger, B. Dumont, U. Ellwanger, J. Gunion, and S. Kraml, “Status of invisible Higgs decays,” 1302.5694.
- [43] P. P. Giardino, K. Kannike, I. Masina, M. Raidal, and A. Strumia, “The universal Higgs fit,” 1303.3570.
- [44] T. Hambye, “Hidden vector dark matter,” *JHEP* **0901** (2009) 028, 0811.0172.
- [45] F. D’Eramo and J. Thaler, “Semi-annihilation of Dark Matter,” *JHEP* **1006** (2010) 109, 1003.5912.
- [46] M. Hindmarsh and O. Philipsen, “WIMP dark matter and the QCD equation of state,” *Phys.Rev.* **D71** (2005) 087302, hep-ph/0501232.
- [47] K. A. Olive, D. N. Schramm, and G. Steigman, “Limits on New Superweakly Interacting Particles from Primordial Nucleosynthesis,” *Nucl. Phys.* **B180** (1981) 497.
- [48] M. Srednicki, R. Watkins, and K. A. Olive, “Calculations of relic densities in the early universe,” *Nucl. Phys.* **B310** (1988) 693.
- [49] G. Hinshaw, D. Larson, E. Komatsu, D. Spergel, C. Bennett, *et al.*, “Nine-Year Wilkinson Microwave Anisotropy Probe (WMAP) Observations: Cosmological Parameter Results,” 1212.5226.
- [50] C. E. Yaguna, “Large contributions to dark matter annihilation from three-body final states,” *Phys.Rev.* **D81** (2010) 075024, 1003.2730.
- [51] A. Goudelis, B. Herrmann, and O. Stl, “Dark matter in the Inert Doublet Model after the discovery of a Higgs-like boson at the LHC,” 1303.3010.
- [52] L. Lopez Honorez and C. E. Yaguna, “The inert doublet model of dark matter revisited,” *JHEP* **09** (2010) 046, 1003.3125.
- [53] G. Belanger, F. Boudjema, A. Pukhov, and A. Semenov, “micrOMEGAs2.0: A program to calculate the relic density of dark matter in a generic model,” *Comput. Phys. Commun.* **176** (2007) 367–382, hep-ph/0607059.
- [54] G. Belanger, F. Boudjema, A. Pukhov, and A. Semenov, “micrOMEGAs: A program for calculating the relic density in the MSSM,” *Comput. Phys. Commun.* **149** (2002) 103–120, hep-ph/0112278.
- [55] **IceCube** Collaboration, R. Abbasi *et al.*, “Search for Neutrinos from Annihilating Dark Matter in the Direction of the Galactic Center with the 40-String IceCube Neutrino Observatory,” 1210.3557.
- [56] M. Boliev, S. Demidov, S. Mikheyev, and O. Suvorova, “Search for muon signal from dark matter annihilations in the Sun with the Baksan Underground Scintillator Telescope for 24.12 years,” 1301.1138.
- [57] **IceCube** Collaboration, C. H. Ha, “The First Year IceCube-DeepCore Results,” *J.Phys.Conf.Ser.* **375** (2012) 052034, 1201.0801.

- [58] A. Gould, “Resonant Enhancements in WIMP Capture by the Earth,” *Astrophys.J.* **321** (1987) 571.
- [59] M. Asplund, N. Grevesse, and J. Sauval, “The Solar chemical composition,” *Nucl.Phys.* **A777** (2006) 1–4, [astro-ph/0410214](#).
- [60] W. McDonough, *Compositional Model for the Earth’s Core*, vol. 2, p. 547568. Elsevier Ltd, 2003.
- [61] K. Griest and D. Seckel, “Cosmic Asymmetry, Neutrinos and the Sun,” *Nucl. Phys.* **B283** (1987) 681.
- [62] A. Gould, “WIMP distribution in and evaporation from the Sun,” *Astrophys.J.* **321** (1987) 560.
- [63] A. Gould, “Evaporation of WIMPs with arbitrary cross-sections,” *Astrophys. J.* (1989).
- [64] M. Cirelli *et al.*, “Spectra of neutrinos from dark matter annihilations,” *Nucl. Phys.* **B727** (2005) 99–138, [hep-ph/0506298](#).
- [65] G. Belanger, M. Kakizaki, E. K. Park, S. Kraml, and A. Pukhov, “Light mixed sneutrinos as thermal dark matter,” *JCAP* **1011** (2010) 017, [1008.0580](#).
- [66] A. E. Erkoca, M. H. Reno, and I. Sarcevic, “Muon Fluxes From Dark Matter Annihilation,” *Phys. Rev.* **D80** (2009) 043514, [0906.4364](#).
- [67] G. Belanger, F. Boudjema, A. Pukhov, and A. Semenov, “Dark matter direct detection rate in a generic model with micrOMEGAs2.1,” *Comput. Phys. Commun.* **180** (2009) 747–767, [0803.2360](#).
- [68] G. Belanger *et al.*, “Indirect search for dark matter with micrOMEGAs2.4,” *Comput. Phys. Commun.* **182** (2011) 842–856, [1004.1092](#).
- [69] F. Boudjema, A. Semenov, and D. Temes, “Self-annihilation of the neutralino dark matter into two photons or a Z and a photon in the MSSM,” *Phys.Rev.* **D72** (2005) 055024, [hep-ph/0507127](#).
- [70] N. Baro, F. Boudjema, and A. Semenov, “Automatised full one-loop renormalisation of the MSSM. I. The Higgs sector, the issue of  $\tan(\beta)$  and gauge invariance,” *Phys.Rev.* **D78** (2008) 115003, [0807.4668](#).
- [71] N. Baro and F. Boudjema, “Automatised full one-loop renormalisation of the MSSM II: The chargino-neutralino sector, the sfermion sector and some applications,” *Phys.Rev.* **D80** (2009) 076010, [0906.1665](#).
- [72] G. Chalons and A. Semenov, “Loop-induced photon spectral lines from neutralino annihilation in the NMSSM,” *JHEP* **1112** (2011) 055, [1110.2064](#).
- [73] H. Zhao, “Analytical Models For Galactic Nuclei,” *Mon. Not. Roy. Astron. Soc.* **278** (1996) 488–496, [astro-ph/9509122](#).

- [74] J. Lavalley, J. Pochon, P. Salati, and R. Taillet, “Clumpiness of Dark Matter and Positron Annihilation Signal: Computing the odds of the Galactic Lottery,” *Astron. Astrophys.* **462** (2007) 827–848, [astro-ph/0603796](#).
- [75] A. Bottino, F. Donato, N. Fornengo, and S. Scopel, “Implications for relic neutralinos of the theoretical uncertainties in the neutralino nucleon cross-section,” *Astropart.Phys.* **13** (2000) 215–225, [hep-ph/9909228](#).
- [76] J. R. Ellis, K. A. Olive, and C. Savage, “Hadronic Uncertainties in the Elastic Scattering of Supersymmetric Dark Matter,” *Phys.Rev.* **D77** (2008) 065026, [0801.3656](#).
- [77] A. Thomas, P. Shanahan, and R. Young, “Strangeness in the nucleon: what have we learned?,” *Nuovo Cim.* **C035N04** (2012) 3–10, [1202.6407](#).
- [78] **Particle Data Group** Collaboration, J. Beringer *et al.*, “Review of Particle Physics (RPP),” *Phys.Rev.* **D86** (2012) 010001.
- [79] **JLQCD** Collaboration, H. Ohki *et al.*, “Nucleon strange quark content from  $N_f = 2 + 1$  lattice QCD with exact chiral symmetry,” [1208.4185](#).
- [80] M. Engelhardt, “Strange quark contributions to nucleon mass and spin from lattice QCD,” *Phys.Rev.* **D86** (2012) 114510, [1210.0025](#).
- [81] **MILC** Collaboration, W. Freeman and D. Toussaint, “The intrinsic strangeness and charm of the nucleon using improved staggered fermions,” [1204.3866](#).
- [82] R. Young and A. Thomas, “Octet baryon masses and sigma terms from an SU(3) chiral extrapolation,” *Phys.Rev.* **D81** (2010) 014503, [0901.3310](#).
- [83] S. Durr, Z. Fodor, T. Hemmert, C. Hoelbling, J. Frison, *et al.*, “Sigma term and strangeness content of octet baryons,” *Phys.Rev.* **D85** (2012) 014509, [1109.4265](#).
- [84] R. Horsley, Y. Nakamura, H. Perlt, D. Pleiter, P. Rakow, *et al.*, “Hyperon sigma terms for 2+1 quark flavours,” *Phys.Rev.* **D85** (2012) 034506, [1110.4971](#).
- [85] A. Semke and M. Lutz, “Strangeness in the baryon ground states,” *Phys.Lett.* **B717** (2012) 242–247, [1202.3556](#).
- [86] P. Shanahan, A. Thomas, and R. Young, “Sigma terms from an SU(3) chiral extrapolation,” [1205.5365](#).
- [87] X.-L. Ren, L. Geng, J. M. Camalich, J. Meng, and H. Toki, “Octet baryon masses in next-to-next-to-next-to-leading order covariant baryon chiral perturbation theory,” [1209.3641](#).
- [88] P. Junnarkar and A. Walker-Loud, “The Scalar Strange Content of the Nucleon from Lattice QCD,” [1301.1114](#).
- [89] G. Bali, P. Bruns, S. Collins, M. Deka, B. Glasle, *et al.*, “Nucleon mass and sigma term from lattice QCD with two light fermion flavors,” *Nucl.Phys.* **B866** (2013) 1–25, [1206.7034](#).

- [90] A. Belyaev, N. D. Christensen, and A. Pukhov, “CalcHEP 3.4 for collider physics within and beyond the Standard Model,” 1207.6082.
- [91] A. Djouadi, “The Anatomy of electro-weak symmetry breaking. I: The Higgs boson in the standard model,” *Phys.Rept.* **457** (2008) 1–216, hep-ph/0503172.
- [92] A. Djouadi, “The Anatomy of electro-weak symmetry breaking. II. The Higgs bosons in the minimal supersymmetric model,” *Phys.Rept.* **459** (2008) 1–241, hep-ph/0503173.
- [93] A. Djouadi, J. Kalinowski, and M. Spira, “HDECAY: A Program for Higgs boson decays in the standard model and its supersymmetric extension,” *Comput.Phys.Commun.* **108** (1998) 56–74, hep-ph/9704448.
- [94] P. Baikov and K. Chetyrkin, “Higgs Decay into Hadrons to Order  $\alpha^5(s)$ ,” *Phys.Rev.Lett.* **97** (2006) 061803, hep-ph/0604194.
- [95] P. Bechtle, O. Brein, S. Heinemeyer, G. Weiglein, and K. E. Williams, “HiggsBounds 2.0.0: Confronting Neutral and Charged Higgs Sector Predictions with Exclusion Bounds from LEP and the Tevatron,” *Comput.Phys.Commun.* **182** (2011) 2605–2631, 1102.1898.
- [96] G. B. *et al*, “Implementaion of new physics models in micrOMEGAs.” in preparation.
- [97] G. Belanger, N. D. Christensen, A. Pukhov, and A. Semenov, “SLHAplus: a library for implementing extensions of the standard model,” *Comput.Phys.Commun.* **182** (2011) 763–774, 1008.0181.
- [98] M. S. Carena, M. Olechowski, S. Pokorski, and C. Wagner, “Electroweak symmetry breaking and bottom - top Yukawa unification,” *Nucl.Phys.* **B426** (1994) 269–300, hep-ph/9402253.
- [99] D. M. Pierce, J. A. Bagger, K. T. Matchev, and R.-j. Zhang, “Precision corrections in the minimal supersymmetric standard model,” *Nucl. Phys.* **B491** (1997) 3–67, hep-ph/9606211.
- [100] F. Boudjema and A. Semenov, “Measurements of the SUSY Higgs selfcouplings and the reconstruction of the Higgs potential,” *Phys.Rev.* **D66** (2002) 095007, hep-ph/0201219.
- [101] M. S. Carena, M. Quiros, and C. Wagner, “Effective potential methods and the Higgs mass spectrum in the MSSM,” *Nucl.Phys.* **B461** (1996) 407–436, hep-ph/9508343.
- [102] B. Allanach, C. Balazs, G. Belanger, M. Bernhardt, F. Boudjema, *et al.*, “SUSY Les Houches Accord 2,” *Comput.Phys.Commun.* **180** (2009) 8–25, 0801.0045.
- [103] F. Mahmoudi, “SuperIso v2.3: A Program for calculating flavor physics observables in Supersymmetry,” *Comput.Phys.Commun.* **180** (2009) 1579–1613, 0808.3144.

- [104] **FlaviaNet Working Group on Kaon Decays** Collaboration, M. Antonelli *et al.*, “Precision tests of the Standard Model with leptonic and semileptonic kaon decays,” 0801.1817.
- [105] A. Akeroyd and F. Mahmoudi, “Constraints on charged Higgs bosons from  $D(s)^\pm \rightarrow \mu^\pm \nu$  and  $D(s)^\pm \rightarrow \tau^\pm \nu$ ,” *JHEP* **0904** (2009) 121, 0902.2393.
- [106] **Heavy Flavor Averaging Group** Collaboration, Y. Amhis *et al.*, “Averages of B-Hadron, C-Hadron, and tau-lepton properties as of early 2012,” 1207.1158.
- [107] G. Belanger, F. Boudjema, C. Hugonie, A. Pukhov, and A. Semenov, “Relic density of dark matter in the NMSSM,” *JCAP* **0509** (2005) 001, hep-ph/0505142.
- [108] T. Hahn and M. Perez-Victoria, “Automatized one loop calculations in four-dimensions and D-dimensions,” *Comput.Phys.Commun.* **118** (1999) 153–165, hep-ph/9807565.
- [109] F. Mahmoudi, S. Heinemeyer, A. Arbey, A. Bharucha, T. Goto, *et al.*, “Flavour Les Houches Accord: Interfacing Flavour related Codes,” *Comput.Phys.Commun.* **183** (2012) 285–298, 1008.0762.
- [110] B. C. Allanach, “SOFTSUSY: a program for calculating supersymmetric spectra,” *Comput. Phys. Commun.* **143** (2002) 305–331, hep-ph/0104145.
- [111] W. Porod, “SPHeno, a program for calculating supersymmetric spectra, SUSY particle decays and SUSY particle production at e+ e- colliders,” *Comput. Phys. Commun.* **153** (2003) 275–315, hep-ph/0301101.
- [112] F. E. Paige, S. D. Protopopescu, H. Baer, and X. Tata, “ISAJET 7.69: A Monte Carlo event generator for pp, anti-p p, and e+e- reactions,” hep-ph/0312045.
- [113] A. Djouadi, M. Muhlleitner, and M. Spira, “Decays of supersymmetric particles: The Program SUSY-HIT (SUSpect-SdecaY-Hdecay-InTerface),” *Acta Phys.Polon.* **B38** (2007) 635–644, hep-ph/0609292.
- [114] G. Degrandi, P. Gambino, and P. Slavich, “SusyBSG: A Fortran code for  $BR(B \rightarrow X(s)\gamma)$  in the MSSM with Minimal Flavor Violation,” *Comput.Phys.Commun.* **179** (2008) 759–771, 0712.3265.